# A Game-Based Approach to Distributed Least-Distance Formation Tracking With a Moving Target

Jun Shi, Maojiao Ye, *Senior Member, IEEE*, Lei Ding, *Senior Member, IEEE*, Shengyuan Xu, *Senior Member, IEEE*, and Qing-Long Han, *Fellow, IEEE*

***Abstract*—This article is concerned with game-based distributed least-distance formation tracking with a moving target. More specifically, the agents aim to form a desired shape while enclosing a moving target with a least overall distance. Different from most of the existing results on formation tracking, the key challenge for least-distance formation tracking under consideration is that the distances between the agents and the target are not required to be predefined but are autonomously adjusted by solving a distance optimization problem. In particular, with the target being moving, the distance optimization problem is time-varying. To address this issue, a game-based formulation of distributed least-distance formation tracking is first presented, where first- and second-order integrator-type agents are taken into account, respectively. Then, under the scenario in which all the agents know the position of the moving target, a new distributed Nash equilibrium seeking strategy that can be utilized to achieve distributed least-distance formation is constructed based on gradient search algorithms, regularization techniques and consensus protocols. Moreover, when it is further considered that only a subset of the agents can access the information of the moving target, a leader-following tracking protocol is introduced to estimate unknown information distributively. It is theoretically shown that the proposed strategies can globally steer the agents to form a desired shape while minimizing the overall distance to the moving target. Finally, the effectiveness of the established strategies is verified by, respectively, conducting simulation studies for a network of vehicles and quadrotors.**

***Index Terms*—Game-based formulation, least-distance formation tracking, moving target, Nash equilibrium seeking.**

Received 15 October 2024; accepted 23 March 2025. Date of publication 4 April 2025; date of current version 29 September 2025. This work was supported in part by the National Natural Science Foundation of China (NSFC) under Grant 62222308, Grant 62173181, Grant 62473203, and Grant 62221004 and in part by the Natural Science Foundation of Jiangsu Province, under Grant BK20220139. Recommended by Associate Editor S. Grammatico. *(Corresponding authors: Maojiao Ye; Qing-Long Han.)*

Jun Shi, Maojiao Ye, and Shengyuan Xu are with the School of Automation, Nanjing University of Science and Technology, Nanjing 210094, China (e-mail: juns@njust.edu.cn; ye0003ao@e.ntu.edu.sg; syxu@njust.edu.cn).

Lei Ding is with the College of Automation & the College of Artificial Intellegence, Nanjing 210023, China, and also with the Institute of Advanced Technology, Nanjing University of Posts and Telecommunications, Nanjing 210023, China (e-mail: dl522@163.com).

Qing-Long Han is with the School of Engineering, Swinburne University of Technology, Melbourne, VIC 3122, Australia (e-mail: qhan@swin.edu.au).

Digital Object Identifier 10.1109/TAC.2025.3558136

## I. Introduction

As a core cooperative control issue of multiagent systems [1], [2], [3], [4], [5], [6], formation control [7], [8], [9], has attracted a lot of attention due to its wide applications in the military field (e.g., source seeking [10], monitoring [11], rescuing [12]), the commercial field (e.g., formation flight to reduce fuel consumption [13]), and the civil field (e.g., agricultural coverage tasks [14]). In many practical applications, multiagent systems intend to not only achieve a formation of a predefined shape but also track a possibly moving target (see source seeking as a typical example [10]) by only utilizing the neighboring information exchange, which leads to distributed formation tracking problems. Note that in the existing distributed formation tracking protocol design [15], [16], [17], [18], [19], [20], [21], [22], [23], [24], there is usually a common setting that the desired distances from the agents to the target (convex hull of multiple targets) should be given a priori. However, such predefined distances may not be an optimal choice and how to optimize them to improve the performance of formation tracking protocols has rarely been investigated. In some practical applications such as target enclosing problems, agents may prefer not only to form an expected shape but also to keep as close to the target as possible, which would be beneficial for the success rate of target catching [25], [26], [27]. In such cases, the distances between the agents and the target should be minimized, thus introducing least-distance formation tracking problems. In addition, in real-world environments, not all agents are capable of accessing information of the moving target. Hence, it should be emphasized that in comparison with most of the existing works on formation tracking, distributed least-distance formation tracking is distinct yet challenging and difficult for protocol design and analysis due to 1) the distances between the agents and the target need to be optimized rather than predefined; 2) the distance optimization problem is time-varying with the target being moving; 3) only a subset of agents can have access to the location of the moving target. Therefore, it is a promising issue to develop a new distributed strategy to achieve least-distance formation tracking with a moving target, which motivates the current study. In summary, compared with the existing works, this article has the following contributions and novelties.

1) A new least-distance formation tracking problem with a moving target is formulated from a perspective of game

theory. Different from formation tracking problems that adopt predefined distances [15], [16], [17], [18], [19], [20], in our formulation, the distances between the agents and the moving target can be autonomously adjusted according to the solution of the distance optimization problem, which is useful for practical applications, such as target capturing problems. Different from [25], [26], [27], and [28] that consider a static target, the target considered in this article is moving, resulting in a time-varying optimization problem.

2) New distributed game-based formation tracking protocols are designed for both first- and second-order integrator-type agents to achieve a desired formation while enclosing a moving target with a least overall distance. This is realized by constructing distributed Nash equilibrium seeking strategies based on gradient search algorithms, consensus algorithms and regularization techniques. Moreover, under the scenario in which only a subset of the agents have access to the information of the target, consensus tracking protocols are incorporated into distributed Nash equilibrium seeking strategies to deal with unavailability of the target's information.

3) Different from [29] that only obtains an approximated solution by using penalty-based algorithms, it is theoretically proven that formation and tracking of a moving target at an optimal distance can be simultaneously achieved. Moreover, sufficient conditions to ensure the effectiveness of the proposed methods are provided. In particular, the proposed methods do not require any restrictions on the moving speed of the target, implying that a fast-moving target can be allowed.

*Related works:* Formation tracking has been a hot research topic in the past two decades. Formation tracking protocols, which can steer networked marine surface vehicles to achieve predefined-time formation tracking, were developed [16]. Event-triggered strategies were proposed to achieve communication-efficient formation stabilization and tracking for Euler-Lagrange systems [19]. For multiple manipulators systems, finite-time time-varying formation tracking protocols were investigated [21]. In [22], leader–follower formation tracking protocols were established for multiple quadrotors. Moreover, for nonlinear quadrotors with parameter uncertainties and external disturbances, robust formation tracking protocols were proposed [23]. Hua et al. [24] studied distributed time-varying output formation tracking of heterogeneous linear systems. Some efforts have also been made to deal with circle formation tracking problems, in which the agents intend to travel along a common circle of a predefined radius centered at the dynamic target, and achieve any desired spacing pattern along the circle. For example, a strategy was proposed to stabilize agents to a circular motion tracking a time-varying center [30]. In addition, circle formation control with an unknown moving target [31] and a moving target with unknown bounded velocity [32] were considered. Moreover, circular formation control of multiple nonholonomic vehicles without global position measurements was considered [33]. However, the aforementioned works achieved the formation with predefined distances/offsets to the target (convex hull of multiple targets), indicating that the distances between the agents and the target (convex hull of multiple targets) might not be optimized.

To realize optimal formation tracking, the formation problem of Euler-Lagrange systems was investigated [28], in which the agents need to achieve distributed formation and optimization simultaneously. However, the distributed optimization problem is time-invariant, indicating that it can not be applied to deal with formation tracking problems with a moving target. In [29], the agents were involved in a formation problem and a time-varying quadratic distributed optimization problem for which a penalty-based protocol is proposed. However, by utilizing the penalty-based approach, only an approximated solution was derived by adopting large penalty parameters. Inspired by the above observations, this article aims to propose a game-based approach to solving distributed least-distance formation tracking problems, by which both formation and tracking of a moving target with an optimal distance can be achieved.

Though game-based approaches to formation control of multi-agent systems have been investigated by some works (e.g., [34], [35], [36], and [37]), most of them do not take distance optimization into consideration. Though least-distance formation has been considered in [25], [26], and [27], the target is considered to be static. With the target being moving, the distance optimization problem becomes a time-varying one, making the problem much more challenging. In addition, various distributed Nash equilibrium seeking strategies have been developed for aggregative games, general normal form noncooperative games and multicluster games [38], [39], [40], [41], [42], [43]. However, it is worth pointing out that, to the best of the authors' knowledge, decision-making problems involving both games and time-varying distributed optimization problems have rarely been investigated. With the objective of enclosing a moving target at the least overall distance, the formation tracking problem is coupled with a time-varying quadratic distributed optimization problem. In this regard, this article also provides new insights into the design and analysis of distributed Nash equilibrium-seeking strategies involving not only local objectives but also time-varying global objectives.

*Article organization:* The rest of this article is organized as follows. Section II introduces the notation and some useful preliminaries. The problem we aim to solve is formulated in Section III. Section IV presents the main strategies and the associated stability analysis. Numerical studies of the proposed methods are given in Section V. Finally, Section VI concludes this article.

## II. Notations and Preliminaries

### A. Notations

In this article, $\mathbb{R}$ and $\mathbb{R}^N$ denote the real number set and $N$-dimensional real column vector set, respectively. Moreover, $\text{diag}\{h_i\}_{i\in\{1,2,\ldots,N\}}$ denotes an $N \times N$-dimensional diagonal matrix with $h_i \in \mathbb{R}$ being the $i$th diagonal element and $\text{diag}\{h_{ij}\}_{i,j\in\{1,2,\ldots,N\}}$ denotes an $N^2 \times N^2$-dimensional diagonal matrix with the diagonal elements being $h_{11}, h_{12}, \ldots, h_{1N}, h_{21}, \ldots, h_{NN}$, respectively. For a symmetric real matrix $\Gamma$, $\lambda_{\min}(\Gamma)$ and $\lambda_{\max}(\Gamma)$ denote the minimum and maximum eigenvalues of $\Gamma$, respectively. The minimum and maximum values of real numbers $q_i$ for $i \in \{1, 2, \ldots, N\}$ are denoted as $\min_{i\in\{1,2,\ldots,N\}}\{q_i\}$ and $\max_{i\in\{1,2,\ldots,N\}}\{q_i\}$, respectively. A matrix with its $(i, j)$th entry being $h_{ij}$ is denoted as $[h_{ij}]_{i,j\in\{1,2,\ldots,N\}}$. $[h_i]_{vec}$ for $i \in \{1, 2, \ldots, N\}$ denotes a column vector whose elements are $h_1, h_2, \ldots, h_N$, successively. In addition, $\otimes$ denotes the Kronecker product and $\|\cdot\|$ denotes the Euclidean norm of vectors or the induced 2-norm for matrices.

$\mathbf{0}_N$ ($\mathbf{1}_N$) represents an $N$-dimensional column vector with all elements being equal to 0 (1) and $I_N$ is an $N \times N$ identity matrix. The notation $s_1 \overset{a.e.}{=} (\overset{a.e.}{\leq}) s_2$ means that $s_1$ is equal (less than or equal) to $s_2$ almost everywhere.

## B. Algebraic Graph Theory

A graph $\mathcal{G}$ is described by $\mathcal{G}(\mathcal{N}, \mathcal{E})$, in which $\mathcal{N} = \{1, 2, \ldots, N\}$ represents the set of nodes and $\mathcal{E} \subseteq \mathcal{N} \times \mathcal{N}$ represents the set of edges. The elements of $\mathcal{E}$ are given by $(i, j)$, which stands for an edge from node $i$ to node $j$. Let $a_{ji}$ be the weight on edge $(i, j) \in \mathcal{E}$. If there is an edge from node $i$ to node $j$, $a_{ji} > 0$, otherwise, $a_{ji} = 0$. Moreover, $a_{ii} = 0$ holds in this article. For undirected graphs, $a_{ij} = a_{ji}, \forall i, j \in \mathcal{N}$. A directed path from $i_{j_1}$ to $i_{j_k}$ is a sequence of edges of the form $(i_{j_1}, i_{j_2}), (i_{j_2}, i_{j_3}), \ldots, (i_{j_{k-1}}, i_{j_k})$. An undirected path in undirected graphs is defined analogously. A directed graph is strongly connected if there exists a directed path from every node to every other node. In addition, an undirected graph is connected if there is an undirected path between any pair of distinct nodes. The adjacency matrix associated with graph $\mathcal{G}$ is denoted as $\mathcal{A} = [a_{ij}]_{i,j\in\mathcal{N}}$. Then, $\mathcal{L} = \mathcal{D} - \mathcal{A}$, where $\mathcal{D} = \operatorname{diag}\{\sum_{j=1}^{N} a_{ij}\}_{i\in\mathcal{N}}$, is called the Laplacian matrix of graph $\mathcal{G}$. Note that $\mathcal{L}\mathbf{1}_N = \mathbf{0}_N$ [44]. The weighted in-degree and out-degree of node $i$ are defined as $d_{in}^i = \sum_{j=1}^{N} a_{ij}$ and $d_{\text{out}}^i = \sum_{j=1}^{N} a_{ji}$, respectively. A digraph $\mathcal{G}$ is weight-balanced if $d_{\text{in}}^i = d_{\text{out}}^i$ for all $i \in \mathcal{N}$. Moreover, the following statements are equivalent: 1) $\mathbf{1}_N^T \mathcal{L} = \mathbf{0}_N^T$; 2) the digraph $\mathcal{G}$ is weight-balanced; 3) $\mathcal{L} + \mathcal{L}^T$ is positive semidefinite.

In addition, if the digraph $\mathcal{G}$ is strongly connected and weight-balanced, 0 is an eigenvalue of both $\mathcal{L}$ and $\mathcal{L} + \mathcal{L}^T$.

In this article, it is considered that the agents communicate with each other via a directed communication graph $\mathcal{G}$ that satisfies the following assumption.

*Assumption 1:* The directed communication graph $\mathcal{G}$ is strongly connected.

Let $\mathcal{K} = \mathcal{L} + D_0$, where $D_0$ is a nonnegative diagonal matrix who has at least one positive diagonal element. Then, the following lemma holds.

*Lemma 1:* [44, Lemma 2.4] Under Assumption 1, there is a positive diagonal matrix $\mathcal{P} = \operatorname{diag}\{p_i\}_{i\in\mathcal{N}}$ such that $\mathcal{P}\mathcal{K} + \mathcal{K}^T\mathcal{P} = \mathcal{Q}$, where $\mathcal{Q}$ is a symmetric positive definite matrix.

*Remark 1:* It should be pointed out that exact values of $\mathcal{P}$ and $\mathcal{Q}$ are not utilized in the control design of this article, and hence, their choices are not discussed here. Interested readers are referred to [44, Lemma 2.5] and many other references for their calculations.

## C. Game Theory

Consider a game with $N$ players, labeled from 1 to $N$, successively. The objective function of player $i$ is defined as $f_i(\mathbf{x})$, where $\mathbf{x} = [x_1^T, x_2^T, \ldots, x_N^T]^T \in \mathbb{R}^{mN}$, $x_i \in \mathbb{R}^m$ is the action of player $i$, and $m \geq 1$ is a positive integer. Each player $i$ aims to solve

$$\min_{x_i\in\mathbb{R}^m} \quad f_i(x_i, \mathbf{x}_{-i}), \ i \in \mathcal{N} \tag{1}$$

where $\mathbf{x}_{-i} = [x_1^T, x_2^T, \ldots, x_{i-1}^T, x_{i+1}^T, \ldots, x_N^T]^T$ and $f_i(\mathbf{x})$ is written as $f_i(x_i, \mathbf{x}_{-i})$ for presentation clarity.

*Definition 1 (See [45]):* Nash equilibrium is an action profile on which no player can decrease its cost by unilaterally changing its own action, i.e., an action profile $\mathbf{x}^* = (x_i^*, \mathbf{x}_{-i}^*) \in \mathbb{R}^{mN}$ is the Nash equilibrium if

$$f_i(x_i^*, \mathbf{x}_{-i}^*) \leq f_i(x_i, \mathbf{x}_{-i}^*) \qquad \forall x_i \in \mathbb{R}^m, i \in \mathcal{N}. \tag{2}$$

## D. Monotonicity

The following monotonicity related definitions are adopted from [46].

A mapping $\mathcal{F} : \mathbb{R}^{mN} \to \mathbb{R}^{mN}$ is monotone if for all $\mathbf{x}, \mathbf{z} \in \mathbb{R}^{mN}$, $(\mathcal{F}(\mathbf{x}) - \mathcal{F}(\mathbf{z}))^T(\mathbf{x} - \mathbf{z}) \geq 0$. It is strictly monotone if the inequality is strict for any $\mathbf{x} \neq \mathbf{z}$. Besides, $\mathcal{F}$ is strongly monotone if for all $\mathbf{x}, \mathbf{z} \in \mathbb{R}^{mN}$, there exists a positive constant $\varepsilon$ such that $(\mathcal{F}(\mathbf{x}) - \mathcal{F}(\mathbf{z}))^T(\mathbf{x} - \mathbf{z}) \geq \varepsilon\|\mathbf{x} - \mathbf{z}\|^2$.

# III. Problem Formulation

In what follows, the considered formation tracking problem is first presented. Then, a game-based formulation of the problem is given, followed by its analytical investigation.

## A. Least-Distance Formation Tracking Problem

Consider a network of $N$ agents that are governed by

$$x_i^{(n)}(t) = u_i(t), \quad i \in \mathcal{N} \tag{3}$$

where $x_i \in \mathbb{R}^m$ is the position of agent $i$ and $u_i$ is the control input. Moreover, $x_i^{(n)}$ is the $n$th order time derivative of $x_i$. In this article, $n = 1$ and $n = 2$ will be successively considered.

Suppose that the agents intend to track a moving target with a desired shape at a least overall distance to the target (i.e., least distance formation tracking). To be more specific, the definition of least distance formation tracking is given as follows.

*Definition 2:* (Least-distance formation tracking) Let $r(t) \in \mathbb{R}^m$ be the position vector of the moving target and $d_i \in \mathbb{R}^n$ be the predefined desired displacement vector of agent $i$. Then,

1) For $n = 1$, the least-distance formation tracking is achieved, if
   a) for $\forall i, j \in \mathcal{N}$, $\lim_{t\to\infty}\big((x_i(t) - d_i) - (x_j(t) - d_j)\big) = \mathbf{0}_m$, indicating that the formation of the desired shape is achieved;
   b) for $\forall i \in \mathcal{N}$, $\lim_{t\to\infty} \mathbf{x}(t) = \min_{\mathbf{x}(t)\in\mathcal{M}} \sum_{i=1}^{N} \|x_i(t) - r(t)\|^2$, where $\mathcal{M} = \{\mathbf{x} \in \mathbb{R}^{mN} | (x_i - d_i) - (x_j - d_j) = \mathbf{0}_m \ \ \forall i, j \in \mathcal{N}\}$, indicating that the overall distance from agents to the moving target is minimized.
2) For $n = 2$, the least-distance formation tracking is achieved, if
   a) for $\forall i, j \in \mathcal{N}$, $\lim_{t\to\infty}\big((x_i(t) - d_i) - (x_j(t) - d_j)\big) = \mathbf{0}_m$, and $\lim_{t\to\infty}(v_i(t) - \dot{r}(t)) = \mathbf{0}_m$, in which $v_i = \dot{x}_i$;
   b) for $\forall i \in \mathcal{N}$, $\lim_{t\to\infty} \mathbf{x}(t) = \min_{\mathbf{x}(t)\in\mathcal{M}} \sum_{i=1}^{N} \|x_i(t) - r(t)\|^2$.

Therefore, the objective of the article is to design distributed control inputs $u_i$, $i \in \mathcal{N}$, for the agents to achieve the least-distance formation tracking.

*Remark 2:* Formation control has wide applications in various fields. In traditional formation tracking problems, the goal is to achieve $\lim_{t\to\infty}(x_i(t) - e_i - r(t)) = \mathbf{0}_m$, in which $e_i$ is the desired offset of agent $i$ to the target [16], [18], [19], [20]. However, such predefined offsets may not be an optimal choice and how to optimize them to improve the performance of formation tracking protocols has rarely been investigated. In addition, in many situations (e.g., target enclosing and catching), it is important to shrink the surrounding circle to capture the target. Motivated by the above observations, this article aims to 1) develop formation tracking protocols, in which the target can be moving and the distance to the target is optimized; 2) achieve simultaneous formation tracking and global time-varying optimization. With the above objectives, the considered least-distance formation tracking problem has two distinct features compared with traditional formation tracking problems. 1) Not only $\lim_{t\to\infty}\left((x_i(t)-d_i)-(x_j(t)-d_j)\right)=\mathbf{0}_m \quad \forall i,j\in\mathcal{N}$, but also $\min_{\mathbf{x}(t)}\sum_{i=1}^N\|x_i(t)-r(t)\|^2$ needs to be addressed. 2) The distances between agents and the target are not predefined but autonomously adjusted by solving minimizing $\sum_{i=1}^N\|x_i(t)-r(t)\|^2$. It is worth pointing out that as the target is moving, the time-varying optimization problem further brings difficulties to the design and analysis of the formation tracking protocol.

## B. Game-Based Algorithm for the Least-Distance Formation Tracking Problem

In this section, we follow [25], [26], and [27] to provide a game-based formulation for the considered problem. To achieve the least-distance formation tracking, suppose that each agent in the formation tracking problem is a player in a normal form game, in which the objective of agent $i$ is given by [25], [26], and [27]

$$\min_{x_i\in\mathbb{R}^m} \quad f_i(x_i,\mathbf{x}_{-i})+\frac{\delta(t)}{2}\|x_i-r(t)\|^2, \quad i\in\mathcal{N} \tag{4}$$

for each $t\geq 0$, where $\delta(t)$ is a time-varying, positive, and smooth parameter to be determined later, and $f_i(x_i,\mathbf{x}_{-i})$ is defined as

$$f_i(x_i,\mathbf{x}_{-i})=\frac{1}{2}\sum_{j=1}^N o_{ij}\|(x_i-d_i)-(x_j-d_j)\|^2,\ i\in\mathcal{N} \tag{5}$$

where $o_{ij}=o_{ji}$ is a binary of 0 and 1 and $o_{ii}=0$.

*1) Insight Into the Game Design:* To achieve solely formation, one can associate each agent $i$ with an objective function given in (5), based on which formation can be achieved by solving the following formation game (see, e.g., [25], [26], [27], and [34]):

$$\min_{x_i\in\mathbb{R}^m} \quad f_i(x_i,\mathbf{x}_{-i}), i\in\mathcal{N} \tag{6}$$

with suitably chosen $o_{ij}$, $i,j\in\mathcal{N}$. If this is the case, the Nash equilibria are achieved at

$$F(\mathbf{x})=(\Omega\otimes I_m)(\mathbf{x}-\mathbf{d})=\mathbf{0}_{mN} \tag{7}$$

where $\mathbf{d}=[d_1^T,\ldots,d_N^T]^T$, $F(\mathbf{x})=[\nabla_1^T f_1(\mathbf{x}),\nabla_2^T f_2(\mathbf{x}),\ldots,\nabla_N^T f_N(\mathbf{x})]^T$, $\nabla_i f_i(\mathbf{x})=\frac{\partial f_i(\mathbf{x})}{\partial x_i}$ and

$$\Omega=\begin{bmatrix}\sum_{j=2}^N o_{1j} & -o_{12} & \cdots & -o_{1\,N}\\ -o_{21} & \sum_{j=1,j\neq 2}^N o_{2j} & \cdots & -o_{2\,N}\\ \vdots & \vdots & \ddots & \vdots\\ -o_{N1} & -o_{N2} & \cdots & \sum_{j=1,j\neq N}^N o_{Nj}\end{bmatrix}.$$

For presentation clarity, we follow [47] to utilize a virtual graph termed as *interference graph* to describe the physical interactions among the agents, which is denoted as $\mathcal{G}^I$. The node set of $\mathcal{G}^I$ is $\mathcal{N}$ and the edge set is $\mathcal{E}^I\subseteq\mathcal{N}\times\mathcal{N}$. If $f_i$ directly depends on $x_j$, there is an undirected edge between agent $i$ and $j$ in the interference graph, i.e., $(i,j)\in\mathcal{E}^I$. Moreover, the corresponding weight of this edge is given as $o_{ij}>0$. Otherwise $o_{ij}=0$. In this regard, $\Omega$ defines the Laplacian matrix of $\mathcal{G}^I$.

*Remark 3:* As depicted in Fig. 1, the interference graph captures the physical interactions among agents, indicating the dependence of each agent's objective function on other agents' states. It is worth noting that by allowing the interference graph to be different from the communication graph, the formulated game generalizes the formation games in [34]. In addition, the case in which the interference graph is aligned with the communication graph will also be discussed in this article.

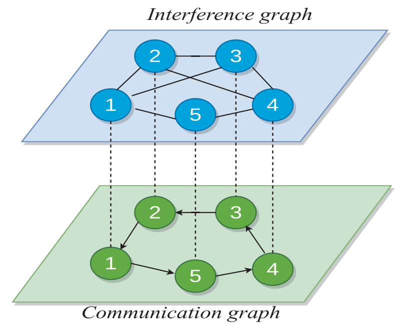


Fig. 1. Illustration of the communication graph and interference graph.

To ensure that the Nash equilibria are associated with the desired formation, it is assumed that the following condition is satisfied.

*Assumption 2:* The interference graph is connected.

It should be pointed out that by Assumption 2, $\Omega$ has only one zero eigenvalue and its corresponding eigenvector is $\mathbf{1}_N$. Hence, at the Nash equilibria, one has $\mathbf{x}-\mathbf{d}=\mathbf{1}_N\otimes c$, where $c\in\mathbb{R}^m$. Hence, the Nash equilibria set of the game corresponding to (6), denoted as $\mathcal{S}=\{\mathbf{x}|\ \mathbf{x}-\mathbf{d}=\mathbf{1}_N\otimes c\}$, is nonempty [26], [27].

However, the game corresponding to (6) can only deal with the formation task. The minimal distance tracking task, i.e., minimization of $\sum_{i=1}^N\|x_i-r(t)\|^2$ remains to be solved. Hence, in (4), $\frac{\delta(t)}{2}||x_i-r(t)||^2$ is added to the game mapping, which can be viewed as a regularization term, to deal with the minimal distance target tracking problem by following [26], [27].

## C. Analysis of the Least-Distance Formation Tracking Game

In what follows, we clarify how to achieve the least-distance formation tracking by the designed game.

By the definition of $f_i(x_i,\mathbf{x}_{-i})$, it can be derived that $F_\delta(\mathbf{x})=F(\mathbf{x})+\delta(t)(\mathbf{x}-\mathbf{r}(t))$, where $\mathbf{r}(t)=\mathbf{1}_N\otimes r(t)$, is strongly monotone for each $t\geq 0$, and thus, game (4) has a unique time-varying Nash equilibrium for each $t\geq 0$, which is denoted by $\mathbf{x}_t^*$.

Let $x_i'=x_i-r(t)$, $\mathbf{x}'=[x_1'^T,x_2'^T,\ldots,x_N'^T]^T$. Then, augmented game (4) and formation game (6) are, respectively, transformed into

$$\min_{x_i'\in\mathbb{R}^m} \quad f_i(x_i',\mathbf{x}_{-i}')+\frac{\delta(t)}{2}\|x_i'\|^2 \tag{8}$$

and

$$\min_{x_i'\in\mathbb{R}^m} \quad f_i(x_i',\mathbf{x}_{-i}') \tag{9}$$

in which

$$f_i(x_i',\mathbf{x}_{-i}')=\frac{1}{2}\sum_{j=1}^N o_{ij}\|(x_i'-d_i)-(x_j'-d_j)\|^2, i\in\mathcal{N} \tag{10}$$

and $\mathbf{x}_{-i}'=[x_1'^T,x_2'^T,\ldots,x_{i-1}'^T,x_{i+1}'^T,\ldots,x_N'^T]^T$. Noting that (5) and (10) have the same expression, it can be concluded by

Assumption 2 that the set of Nash equilibria of the game corresponding to (9), denoted as $\mathcal{S}' = \{\mathbf{x}' | \, \mathbf{x}' - \mathbf{d} = \mathbf{1}_N \otimes c\}$, is nonempty.

Let $F_\delta(\mathbf{x}') = F(\mathbf{x}') + \delta(t)\mathbf{x}'$. According to the strong monotonicity of $F_\delta(\mathbf{x}')$, $\mathbf{x}'^*_t = \mathbf{x}^*_t - \mathbf{r}(t)$ is the unique Nash equilibrium of (8), on which $F_\delta(\mathbf{x}'^*_t) = F(\mathbf{x}'^*_t) + \delta(t)\mathbf{x}'^*_t = \mathbf{0}_{mN}$.

Let $\mathbf{x}^*(t) \in \mathcal{S}$ be the Nash equilibrium that solves

$$\min_{\mathbf{x}\in\mathcal{S}} \quad \|\mathbf{x} - \mathbf{r}(t)\|^2 \tag{11}$$

and let $\mathbf{x}^*_m$ be the least-norm Nash equilibrium in $\mathcal{S}'$. Then, it is obvious that $\mathbf{x}^*_m = \mathbf{x}^*(t) - \mathbf{r}(t)$ by the definition of $\mathbf{x}^*(t)$. By the results in [48] and [49], the following lemmas hold for game (9) and its corresponding augmented game (8).

*Lemma 2:* [48, Lemma 4] Suppose that Assumption 2 holds and $\lim_{t\to\infty}\delta(t) = 0$. Then, $\lim_{t\to\infty}\mathbf{x}'^*_t = \mathbf{x}^*_m$ and $\|\mathbf{x}'^*_t\| \leq \|\mathbf{x}^*_m\|$.

*Lemma 3:* [49, Lemma 2.3] Suppose that Assumption 2 holds and $\lim_{t\to\infty}\delta(t) = 0$. Then,

1) $\dot{\mathbf{x}}'^*_t$ exists almost everywhere;
2) there exists a positive constant $c_x$ such that $\|\dot{\mathbf{x}}'^*_t\| \overset{a.e.}{\leq} c_x \frac{|\dot{\delta}(t)|}{\delta(t)}$ holds.

Based on Lemmas 2 and 3, the following corollary can be derived for game (4) and game (6).

*Corollary 1:* Suppose that Assumption 2 holds, $\lim_{t\to\infty}\delta(t) = 0$, and $\mathbf{r}(t)$ is continuously differentiable. Then

1) $\lim_{t\to\infty}(\mathbf{x}^*_t - \mathbf{x}^*(t)) = \mathbf{0}_{mN}$ and $\|\mathbf{x}^*_t - \mathbf{r}(t)\| \leq \|\mathbf{x}^*(t) - \mathbf{r}(t)\|$;
2) $\dot{\mathbf{x}}^*_t - \dot{\mathbf{r}}(t)$ exists almost everywhere;
3) there exists a positive constant $c_x$ such that $\|\dot{\mathbf{x}}^*_t - \dot{\mathbf{r}}(t)\| \overset{a.e.}{\leq} c_x \frac{|\dot{\delta}(t)|}{\delta(t)}$ holds.

*Remark 4:* According to Corollary 1, least-distance formation tracking can be achieved by seeking the Nash equilibrium of the game corresponding to (4) provided that $\delta(t)$ is decaying to zero.

## IV. Main Results

In what follows, the considered formation tracking problem is first presented. Then, a game-based formulation of the problem is given, followed by its analytical investigation.

### A. First-Order Integrator-Type Systems

In this section, it is considered that the agents' positions are governed by

$$\dot{x}_i = u_i, \quad i \in \mathcal{N}. \tag{12}$$

Moreover, suppose that the following condition is satisfied for the trajectory of the moving target.

*Assumption 3:* The first- and second-order time derivatives of $r(t)$, i.e., $\dot{r}(t)$ and $\ddot{r}(t)$, exist.

In what follows, the case in which the trajectory information of the moving target $r(t)$ and $\dot{r}(t)$ are available to all agents will be addressed in Section IV-A1. Then, this condition is relaxed by supposing that $r(t)$ and $\dot{r}(t)$ are only available to a subset of agents.

***1) Trajectory of the Moving Target is Available to All the Agents:*** With $r(t)$ and $\dot{r}(t)$ available to all agents, $u_i$ can be designed as

$$u_i = -k_1\left(\nabla_i f_i(\mathbf{y}_i) + \delta(t)\,(x_i - r(t))\right) + \dot{r}(t) \tag{13}$$

for $i \in \mathcal{N}$, where $\nabla_i f_i(\mathbf{y}_i) = \frac{\partial f_i(\mathbf{x})}{\partial x_i}|_{\mathbf{x}=\mathbf{y}_i}$ and $\mathbf{y}_i = [y^T_{i1}, \ldots, y^T_{iN}]^T$.

Furthermore, for each $i, j \in \mathcal{N}$, $y_{ij}$ is updated by

$$\dot{y}_{ij} = -\omega(t)\left(\sum_{k=1}^{N} a_{ik}(y_{ij} - y_{kj}) + a_{ij}(y_{ij} - x_j)\right) + \dot{r}(t) \tag{14}$$

where $\omega(t)$ is a time-varying, positive, and smooth parameter. Note that $y_{ij}$ is generated to estimate $x_j$, which may not be directly available to agent $i$ as $f_i(x_i, \mathbf{x}_{-i})$ depends on not only $x_i$ but also $\mathbf{x}_{-i}$.

*Remark 5:* It should be pointed out that $y_{ii}$ can be removed from (14), which gives

$$\dot{y}_{ij} = -\omega(t)\sum_{k=1}^{N} a_{ik}(y_{ij} - y_{kj}) + \dot{r}(t),\ j \in \mathcal{N}\backslash\{i\}$$

where $y_{ii} = x_i$. This modification does not affect the convergence results, and we adopt (14) in the article just for notational convenience of its concatenated vector form. In addition, by adopting the interference graph based information exchange scheme in [47], the communication burden can be further reduced. Interested readers are referred to [47] for more details.

Based on (12)–(14)

$$\begin{cases} \dot{\mathbf{x}} = -k_1\left([\nabla_i f_i(\mathbf{y}_i)]_{\text{vec}} + \delta(t)\,(\mathbf{x} - \mathbf{r}(t))\right) + \dot{\mathbf{r}}(t) \\ \dot{\mathbf{y}} = -\omega(t)(\mathcal{L} \otimes I_{mN} + B_0)(\mathbf{y} - \mathbf{1}_N \otimes \mathbf{x}) + \mathbf{1}_N \otimes \dot{\mathbf{r}}(t) \end{cases} \tag{15}$$

where $\mathbf{y} = [\mathbf{y}^T_1, \ldots, \mathbf{y}^T_N]^T$, $B_0 = \text{diag}\{a_{ij}\}_{i,j\in\mathcal{N}} \otimes I_m$, and $[\nabla_i f_i(\mathbf{y}_i)]_{\text{vec}} = [\nabla^T_1 f_1(\mathbf{y}_1), \ldots, \nabla^T_N f_N(\mathbf{y}_N)]^T$.

Let $\bar{\mathbf{x}} = \mathbf{x} - \mathbf{x}^*_t$ and $\bar{\mathbf{y}} = \mathbf{y} - \mathbf{1}_N \otimes \mathbf{x}$. Then

$$\begin{cases} \dot{\bar{\mathbf{x}}} \overset{a.e.}{=} -k_1\left([\nabla_i f_i(\mathbf{y}_i)]_{\text{vec}} + \delta(t)\,(\mathbf{x} - \mathbf{r}(t))\right) - (\dot{\mathbf{x}}^*_t - \dot{\mathbf{r}}(t)) \\ \dot{\bar{\mathbf{y}}} = -\omega(t)(\mathcal{L} \otimes I_{mN} + B_0)\bar{\mathbf{y}} - \mathbf{1}_N \otimes (\dot{\mathbf{x}} - \dot{\mathbf{r}}(t)). \end{cases} \tag{16}$$

Since the communication graph $\mathcal{G}$ is directed and strongly connected by Assumption 1, there exists a positive diagonal matrix $\mathcal{P}$ such that $\mathcal{P}(\mathcal{L} \otimes I_{mN} + B_0) + (\mathcal{L} \otimes I_{mN} + B_0)^T\mathcal{P} = \mathcal{Q}$, where $\mathcal{Q}$ is a symmetric positive definite matrix by Lemma 1. Based on this result, the following theorem can be derived.

*Theorem 1:* Under Assumptions 1–3, $(\mathbf{x}, \mathbf{y})$ is globally asymptotically convergent to $(\mathbf{x}^*(t), \mathbf{1}_N \otimes \mathbf{x}^*(t))$ given that $\delta(t)$ and $\omega(t)$ are chosen to satisfy

$$\lim_{t\to\infty}\delta(t) = 0, \lim_{t\to\infty}\int_0^t \delta(s)ds = \infty, \lim_{t\to\infty}\frac{|\dot{\delta}(t)|}{\delta^2(t)} = 0$$
$$\delta(t)\lambda_{\min}(\mathcal{Q})\omega(t) \geq \xi(\delta) \tag{17}$$

where $\xi(\delta) = k_1(\max_{i\in\mathcal{N}}\{l_i\})^2 + 4k_1N\|\mathcal{P}\|^2(\sqrt{N}\max_{i\in\mathcal{N}}\{l_i\} + \delta(t))^2 + 2k_1\delta(t)\sqrt{N}\|\mathcal{P}\|\max_{i\in\mathcal{N}}\{l_i\} + \frac{\delta(t)^2 k_1}{2}$ and $l_i = \sqrt{\sum_{j=1,j\neq i}^{N}(o_{ij})^2 + (\sum_{j=1,j\neq i}^{N} o_{ij})^2}$.

*Proof:* Define $V = V_1 + V_2$, where $V_1 = \frac{1}{2}(\mathbf{x} - \mathbf{x}^*_t)^T(\mathbf{x} - \mathbf{x}^*_t)$ and $V_2 = \bar{\mathbf{y}}^T\mathcal{P}\bar{\mathbf{y}}$. Then, it is clear that $V$ is positive definite and radially unbounded with respect to $\mathbf{E}_1 = [(\mathbf{x} - \mathbf{x}^*_t)^T, \bar{\mathbf{y}}^T]^T$. Noting that by (7), one can get that $\|[\nabla_i f_i(\mathbf{y}_i)]_{vec} - F(\mathbf{x})\| \leq \max_{i\in\mathcal{N}}\{l_i\}\|\bar{\mathbf{y}}\|$. Moreover, $\|F(\mathbf{x}) - F(\mathbf{x}^*_t)\| \leq$

$\sqrt{N}\max_{i\in\mathcal{N}}\{l_i\}\|\mathbf{x}-\mathbf{x}_t^*\|$. Hence

$$\begin{aligned}\dot{V}_1 \overset{a.e.}{=} & -k_1(\mathbf{x}-\mathbf{x}_t^*)^T\Big([\nabla_i f_i(\mathbf{y}_i)]_{\text{vec}}+\delta(t)\left(\mathbf{x}-\mathbf{r}(t)\right)\Big)\\ & -(\mathbf{x}-\mathbf{x}_t^*)^T\left(\dot{\mathbf{x}}_t^*-\dot{\mathbf{r}}(t)\right)\\ \overset{a.e.}{=} & -k_1(\mathbf{x}-\mathbf{x}_t^*)^T\Big(([\nabla_i f_i(\mathbf{y}_i)]_{\text{vec}}-F(\mathbf{x}))+(F(\mathbf{x})\\ & -F(\mathbf{x}_t^*))+\delta(t)(\mathbf{x}-\mathbf{x}_t^*)\Big)-(\mathbf{x}-\mathbf{x}_t^*)^T\left(\dot{\mathbf{x}}_t^*-\dot{\mathbf{r}}(t)\right)\\ \overset{a.e.}{\leq} & -\delta(t)k_1\|\mathbf{x}-\mathbf{x}_t^*\|^2+(\delta(t)k_1/4)\|\mathbf{x}-\mathbf{x}_t^*\|^2\\ & +k_1((\max_{i\in\mathcal{N}}\{l_i\})^2/\delta(t))\|\bar{\mathbf{y}}\|^2\\ & +\|\mathbf{x}-\mathbf{x}_t^*\|\|\dot{\mathbf{x}}_t^*-\dot{\mathbf{r}}(t)\|. \end{aligned} \tag{18}$$

In addition

$$\begin{aligned}\dot{V}_2 = & \,\bar{\mathbf{y}}^T\mathcal{P}\left(-\omega(t)(\mathcal{L}\otimes I_{mN}+B_0)\bar{\mathbf{y}}+\mathbf{1}_N\otimes(\dot{\mathbf{r}}(t)-\dot{\mathbf{x}})\right)\\ & +\left(-\omega(t)(\mathcal{L}\otimes I_{mN}+B_0)\bar{\mathbf{y}}+\mathbf{1}_N\otimes(\dot{\mathbf{r}}(t)-\dot{\mathbf{x}})\right)^T\mathcal{P}\bar{\mathbf{y}}\\ = & -\omega(t)\bar{\mathbf{y}}^T\mathcal{Q}\bar{\mathbf{y}}+2k_1\bar{\mathbf{y}}^T\mathcal{P}\left(\mathbf{1}_N\otimes([\nabla_i f_i(\mathbf{y}_i)]_{\text{vec}}\right.\\ & \left.+\delta(t)\left(\mathbf{x}-\mathbf{r}(t)\right))\right). \end{aligned} \tag{19}$$

Moreover

$$\begin{aligned}&\bar{\mathbf{y}}^T\mathcal{P}\Big(\mathbf{1}_N\otimes\left([\nabla_i f_i(\mathbf{y}_i)]_{\text{vec}}+\delta(t)\left(\mathbf{x}-\mathbf{r}(t)\right)\right)\Big)\\ &\leq \delta(t)/8\|\mathbf{x}-\mathbf{x}_t^*\|^2+\sqrt{N}\|\mathcal{P}\|\max_{i\in\mathcal{N}}\{l_i\}\|\bar{\mathbf{y}}\|^2\\ &\quad+(2N\|\mathcal{P}\|^2(\sqrt{N}\max_{i\in\mathcal{N}}\{l_i\}+\delta(t))^2/\delta(t))\|\bar{\mathbf{y}}\|^2. \end{aligned} \tag{20}$$

Hence, by (18)–(20), it can be derived that

$$\begin{aligned}\dot{V}\overset{a.e.}{\leq} & -(\delta(t)k_1/2)\|\mathbf{x}-\mathbf{x}_t^*\|^2-(\omega(t)\lambda_{\min}(\mathcal{Q})\\ & -k_1(\max_{i\in\mathcal{N}}\{l_i\})^2/\delta(t)\\ & -4k_1N\|\mathcal{P}\|^2(\sqrt{N}\max_{i\in\mathcal{N}}\{l_i\}+\delta(t))^2/\delta(t)\\ & -2k_1\sqrt{N}\|\mathcal{P}\|\max_{i\in\mathcal{N}}\{l_i\}\Big)\|\bar{\mathbf{y}}\|^2\\ & +\|\mathbf{x}-\mathbf{x}_t^*\|\|\dot{\mathbf{x}}_t^*-\dot{\mathbf{r}}(t)\|. \end{aligned} \tag{21}$$

Choosing $\omega(t)$ such that $\omega(t)\lambda_{\min}(\mathcal{Q})-\frac{k_1(\max_{i\in\mathcal{N}}\{l_i\})^2}{\delta(t)}-\frac{4k_1N\|\mathcal{P}\|^2(\sqrt{N}\max_{i\in\mathcal{N}}\{l_i\}+\delta(t))^2}{\delta(t)}-2k_1\sqrt{N}\|\mathcal{P}\|\max_{i\in\mathcal{N}}\{l_i\}\geq\frac{\delta(t)k_1}{2}$, one obtains that

$$\dot{V}\overset{a.e.}{\leq}-\frac{\delta(t)k_1}{2}\left(\|\mathbf{x}-\mathbf{x}_t^*\|^2+\|\bar{\mathbf{y}}\|^2\right)+\|\mathbf{x}-\mathbf{x}_t^*\|\|\dot{\mathbf{x}}_t^*-\dot{\mathbf{r}}(t)\|. \tag{22}$$

Recalling the definition of $V$, one has $\min\{\frac{1}{2},\lambda_{\min}(\mathcal{P})\}\|\mathbf{E}_1\|^2\leq V\leq\max\{\frac{1}{2},\lambda_{\max}(\mathcal{P})\}\|\mathbf{E}_1\|^2$. Hence

$$\dot{V}\overset{a.e.}{\leq}-\frac{\delta(t)k_1}{2\max\{\frac{1}{2},\lambda_{\max}(\mathcal{P})\}}V+\sqrt{2V}\|\dot{\mathbf{x}}_t^*-\dot{\mathbf{r}}(t)\|. \tag{23}$$

Let $J=\sqrt{2V}$ and $E(t)=\int_{s=0}^{t}\frac{\delta(s)k_1}{4\max\{\frac{1}{2},\lambda_{\max}(\mathcal{P})\}}\mathrm{d}s$. Then

$$\dot{J}\overset{a.e.}{\leq}-\frac{\delta(t)k_1}{4\max\{\frac{1}{2},\lambda_{\max}(\mathcal{P})\}}J+c_x\frac{|\dot{\delta}(t)|}{\delta(t)} \tag{24}$$

as $\|\dot{\mathbf{x}}_t^*-\dot{\mathbf{r}}(t)\|\overset{a.e.}{\leq}c_x\frac{|\dot{\delta}(t)|}{\delta(t)}$ by Corollary 1. Moreover

$$\frac{\mathrm{d}}{\mathrm{d}t}\left(Je^{E(t)}\right)\overset{a.e.}{\leq}c_x\frac{|\dot{\delta}(t)|}{\delta(t)}e^{E(t)}. \tag{25}$$

Taking integration on both sides of (25) over $[0,T]$, it can be derived that

$$J(T)e^{E(T)}-J(0)\leq\int_0^T c_x\frac{|\dot{\delta}(s)|}{\delta(s)}e^{E(s)}\mathrm{d}s \tag{26}$$

and hence

$$0\leq J(T)\leq e^{-E(T)}J(0)+e^{-E(T)}\int_0^T c_x\frac{|\dot{\delta}(s)|}{\delta(s)}e^{E(s)}\mathrm{d}s. \tag{27}$$

Since $\lim_{t\to\infty}\int_0^t\delta(s)\mathrm{d}s=\infty$, $\lim_{t\to\infty}e^{-E(t)}=0$. Besides, as $\lim_{t\to\infty}\frac{|\dot{\delta}(t)|}{\delta^2(t)}=0$, it can be derived that $\lim_{t\to\infty}e^{-E(t)}\int_0^t c_x\frac{|\dot{\delta}(s)|}{\delta(s)}e^{E(s)}\mathrm{d}s=0$. This indicates that $\lim_{t\to\infty}J(t)=0$.

Thus, $\lim_{t\to\infty}\|\mathbf{x}(t)-\mathbf{x}_t^*\|=0$ and $\lim_{t\to\infty}\|\mathbf{y}(t)-\mathbf{1}_N\otimes\mathbf{x}(t)\|=0$. Moreover, by Corollary 1, $\lim_{t\to\infty}\|\mathbf{x}(t)-\mathbf{x}^*(t)\|=0$, and $\lim_{t\to\infty}\|\mathbf{y}(t)-\mathbf{1}_N\otimes\mathbf{x}^*(t)\|=0$. Hence, the conclusion is derived. □

*Remark 6:* By (27), it can be derived that

$$\begin{aligned}\|\mathbf{x}(t)-\mathbf{x}_t^*\|\leq & \, e^{-E(t)}\sqrt{\max\{1,\lambda_{\max}(2\mathcal{P})\}}\|\mathbf{E}_1(0)\|\\ & +e^{-E(t)}\int_0^t c_x\frac{|\dot{\delta}(s)|}{\delta(s)}e^{E(s)}\mathrm{d}s \end{aligned} \tag{28}$$

indicating that the convergence speed is determined by $\delta(t)$, $k_1$, and $\mathcal{P}$.

In (13)–(14), each agent needs to generate a local estimate on other agents' positions, which may introduce some communication burden. This can be relaxed by defining $o_{ij}=a_{ij}$, which indicates that each agent $i$'s objective function $f_i(x_i,\mathbf{x}_{-i})$ is only dependent on $x_i$ and its neighbors' positions. If this is the case, $u_i$ can be designed as

$$u_i=-k_1\Big(\nabla_i f_i(\mathbf{x})+\delta(t)\left(x_i-r(t)\right)\Big)+\dot{r}(t) \tag{29}$$

for $i\in\mathcal{N}$, if $r(t)$ and $\dot{r}(t)$ are available to all agents.

Then, the following corollary can be derived for (29).

*Corollary 2:* Suppose that Assumptions 1 and 3 hold and graph $\mathcal{G}$ is weight-balanced. Then

$$\lim_{t\to\infty}\|\mathbf{x}(t)-\mathbf{x}^*(t)\|=0 \tag{30}$$

if $\delta(t)$ is chosen such that $\lim_{t\to\infty}\delta(t)=0,\lim_{t\to\infty}\int_0^t\delta(s)ds=\infty,\lim_{t\to\infty}\frac{|\dot{\delta}(t)|}{\delta^2(t)}=0$.

*Proof:* As $o_{ij}=a_{ij}$ and $\mathcal{G}$ is a weight-balanced strongly connected graph, one has

$$(\mathbf{x}-\mathbf{x}_t^*)^T(F(\mathbf{x})-F(\mathbf{x}_t^*))=(\mathbf{x}-\mathbf{x}_t^*)^T\frac{(\mathcal{L}+\mathcal{L}^T)_\otimes}{2}(\mathbf{x}-\mathbf{x}_t^*) \tag{31}$$

where $(\mathcal{L}+\mathcal{L}^T)_\otimes=(\mathcal{L}+\mathcal{L}^T)\otimes I_m$. Hence

$$\lambda_{\min}\left(\frac{\mathcal{L}+\mathcal{L}^T}{2}\right)\|\mathbf{x}-\mathbf{x}_t^*\|^2\leq(\mathbf{x}-\mathbf{x}_t^*)^T\left(F(\mathbf{x})-F(\mathbf{x}_t^*)\right). \tag{32}$$

As $\lambda_{\min}(\frac{\mathcal{L}+\mathcal{L}^T}{2})=0$ under the weight-balanced and connected digraph, it can be derived that $(\mathbf{x}-\mathbf{x}_t^*)^T(F(\mathbf{x})-F(\mathbf{x}_t^*))\geq 0$.

Defining $V=\frac{1}{2}(\mathbf{x}-\mathbf{x}_t^*)^T(\mathbf{x}-\mathbf{x}_t^*)$, one has

$$\dot{V}\overset{a.e.}{=}-k_1(\mathbf{x}-\mathbf{x}_t^*)^T\left(F(\mathbf{x})+\delta(t)\left(\mathbf{x}-\mathbf{r}(t)\right)\right)$$

$$+\left(\mathbf{x}-\mathbf{x}_t^*\right)^T\left(\dot{\mathbf{x}}_t^*-\dot{\mathbf{r}}(t)\right)$$
$$\overset{a.e.}{\leq} -\delta(t)k_1\|\mathbf{x}-\mathbf{x}_t^*\|^2+\|\mathbf{x}-\mathbf{x}_t^*\|\|\dot{\mathbf{x}}_t^*-\dot{\mathbf{r}}(t)\|. \quad (33)$$

The remaining analysis follows that the proof of Theorem 1 and hence, is omitted here. □

In Theorem 1 and Corollary 2, it is considered that the trajectory information of the moving target is known to all agents. However, in practical situations, this is hard/costly to be achieved. To relax it, it is further considered that only a subset of agents know the trajectory information of the moving target.

***2) Trajectory of the Moving Target is Available to Only a Subset of Agents:*** In this section, it is assumed that the trajectory information of the moving target is known to only a subset of the agents. If this is the case, the control law in (13) is not applicable. To deal with unavailability of $r(t)$ and $\dot{r}(t)$, we suppose that each agent would generate local estimates of $r(t)$ and $\dot{r}(t)$. Based on this idea, the control input $u_i$ for each agent $i$ is designed as

$$\begin{cases} u_i=-k_1\left(\nabla_i f_i(\mathbf{y}_i)+\delta(t)\left(x_i-\theta_i(t)\right)\right)+\gamma_i(t)\\ \dot{y}_{ij}=-\omega(t)\left(\sum_{k=1}^N a_{ik}(y_{ij}-y_{kj})+a_{ij}(y_{ij}-x_j)\right)+\gamma_i(t)\end{cases} \quad (34)$$

for $i,j\in\mathcal{N}$, where $\theta_i(t)\in\mathbb{R}^m$ and $\gamma_i(t)\in\mathbb{R}^m$ are the estimates of $r(t)$ and $\dot{r}(t)$, respectively.

Let $\mathbf{p}_i=[\theta_i^T(t),\gamma_i^T(t)]^T$, $\tilde{\mathbf{r}}_1=[r(t)^T,\dot{r}(t)^T]^T$ and $\varphi_1(t)=\operatorname{diag}\{\alpha(t),\beta(t)\}\otimes I_m$, where $\alpha(t)$ and $\beta(t)$ are time-varying, positive, and smooth parameters. Then, for each $i\in\mathcal{N}$, $\mathbf{p}_i$ is generated by

$$\dot{\mathbf{p}}_i=\frac{1}{\sum_{j=1}^N a_{ij}+\eta_i}\sum_{j=1}^N a_{ij}\left(\dot{\mathbf{p}}_j-\varphi_1(t)\left(\mathbf{p}_i-\mathbf{p}_j\right)\right)+\frac{\eta_i}{\sum_{j=1}^N a_{ij}+\eta_i}\left(\dot{\tilde{\mathbf{r}}}_1-\varphi_1(t)\left(\mathbf{p}_i-\tilde{\mathbf{r}}_1\right)\right) \quad (35)$$

where $\eta_i=1$ indicates that agent $i$ can receive/observe the information of the moving target (e.g., $r(t),\dot{r}(t)$), and vice versa, $\eta_i=0$. To ensure that the target's information can be estimated, we need the following assumption.

*Assumption 4:* There exists at least one agent that can access the information of the moving target, i.e., $\exists i$ such that $\eta_i=1$.

*Remark 7:* As the target is moving, a consensus tracking algorithm (35) is utilized to generate local estimates of $r(t)$, $\dot{r}(t)$, which is similar to [50]. In addition, it is noted that in (35), the moving target acts as a "leader" and the agents act as "followers" trying to track the moving target.

By (12) and (34), one can get that

$$\begin{cases}\dot{\mathbf{x}}=-k_1\left([\nabla_i f_i(\mathbf{y}_i)]_{vec}+\delta(t)\left(\mathbf{x}-\Theta\right)\right)+\Upsilon\\ \dot{\mathbf{y}}=-\omega(t)(\mathcal{L}\otimes I_{mN}+B_0)(\mathbf{y}-\mathbf{1}_N\otimes\mathbf{x})+\mathbf{1}_N\otimes\Upsilon\end{cases} \quad (36)$$

where $\Theta=[\theta_1^T,\theta_2^T,\ldots,\theta_N^T]^T$ and $\Upsilon=[\gamma_1^T,\gamma_2^T,\ldots,\gamma_N^T]^T$.

Let $\bar{\Theta}=\Theta(t)-\mathbf{r}(t)$ and $\bar{\Upsilon}=\Upsilon(t)-\dot{\mathbf{r}}(t)$, one has

$$\begin{cases}\dot{\bar{\mathbf{x}}}\overset{a.e.}{=}-k_1\left([\nabla_i f_i(\mathbf{y}_i)]_{vec}+\delta(t)\left(\mathbf{x}-\mathbf{r}(t)\right)\right)\\ \quad -(\dot{\mathbf{x}}_t^*-\dot{\mathbf{r}}(t))+\delta(t)\bar{\Theta}+\bar{\Upsilon}\\ \dot{\bar{\mathbf{y}}}=-\omega(t)(\mathcal{L}\otimes I_{mN}+B_0)\bar{\mathbf{y}}-\mathbf{1}_N\otimes\dot{\mathbf{x}}+\mathbf{1}_N\otimes\Upsilon.\end{cases} \quad (37)$$

Then, multiplying both sides of (35) by $\sum_{i=1}^j a_{ij}+\eta_i$ gives $(\sum_{i=1}^j a_{ij}+\eta_i)\dot{\mathbf{p}}_i=\sum_{j=1}^N a_{ij}(\dot{\mathbf{p}}_j-\varphi_1(t)(\mathbf{p}_i-\mathbf{p}_j))+\eta_i(\dot{\tilde{\mathbf{r}}}_1-\varphi_1(t)(\mathbf{p}_i-\tilde{\mathbf{r}}_1))$. Hence

$$(\mathcal{L}\otimes I_m+\Xi)(\dot{\Theta}-\dot{\mathbf{r}}(t))=-\alpha(t)(\mathcal{L}\otimes I_m+\Xi)(\Theta-\mathbf{r}(t))$$
$$(\mathcal{L}\otimes I_m+\Xi)(\dot{\Upsilon}-\ddot{\mathbf{r}}(t))=-\beta(t)(\mathcal{L}\otimes I_m+\Xi)(\Upsilon-\dot{\mathbf{r}}(t))$$

where $\Xi=\operatorname{diag}\{\eta_i\}_{i\in\mathcal{N}}\otimes I_m$.

Define $\Phi_1=(\mathcal{L}\otimes I_m+\Xi)\bar{\Theta}$ and $\Phi_2=(\mathcal{L}\otimes I_m+\Xi)\bar{\Upsilon}$. Then

$$\dot{\Phi}_1=-\alpha(t)\Phi_1,\quad \dot{\Phi}_2=-\beta(t)\Phi_2. \quad (38)$$

Note that as the communication graph $\mathcal{G}$ is strongly connected, $\mathcal{L}\otimes I_m+\Xi$ is nonsingular under Assumption 4. Hence, $\|\bar{\Theta}\|\leq\chi\|\Phi_1\|$ and $\|\bar{\Upsilon}\|\leq\chi\|\Phi_2\|$, where $\chi=\|(\mathcal{L}\otimes I_m+\Xi)^{-1}\|$ is a positive constant. Based on this observation, the following result can be derived for the least-distance formation tracking protocol in (34)–(35).

*Theorem 2:* Under Assumptions 1–4, $(\mathbf{x},\mathbf{y},\Theta,\Upsilon)$ is globally asymptotically convergent to $(\mathbf{x}^*(t),\mathbf{1}_N\otimes\mathbf{x}^*(t),\mathbf{r}(t),\dot{\mathbf{r}}(t))$ given that

$$\lim_{t\to\infty}\delta(t)=0,\ \lim_{t\to\infty}\int_0^t\delta(s)\mathrm{d}s=\infty,\ \lim_{t\to\infty}\frac{|\dot{\delta}(t)|}{\delta^2(t)}=0$$
$$\delta(t)\omega(t)\lambda_{\min}(\mathcal{Q})\geq\Gamma_1(\delta),\alpha(t)\geq\Gamma_2(\delta),\delta(t)\beta(t)\geq\Gamma_3(\delta) \quad (39)$$

where $\Gamma_1(\delta)=2\delta(t)k_1\|\mathcal{P}\|\sqrt{N}\max_{i\in\mathcal{N}}\{l_i\}+2k_1(\max_{i\in\mathcal{N}}\{l_i\})^2+8k_1N\|\mathcal{P}\|^2(\sqrt{N}\max_{i\in\mathcal{N}}\{l_i\}+\delta(t))^2+\frac{\delta(t)^2k_1}{2}$, $\Gamma_2(\delta)=2\delta(t)\chi^2+\delta(t)k_1N\chi^2\|\mathcal{P}\|^2+\frac{\delta(t)^2k_1}{2}$, and $\Gamma_3(\delta)=\frac{2\chi^2}{k_1}+\frac{\delta(t)^2k_1}{2}$.

*Proof:* Define $V=V_1+V_2+V_3+V_4$, where $V_1=\frac{1}{2}(\mathbf{x}-\mathbf{x}_t^*)^T(\mathbf{x}-\mathbf{x}_t^*)$, $V_2=\bar{\mathbf{y}}^T\mathcal{P}\bar{\mathbf{y}}$, $V_3=\frac{1}{2}\Phi_1^T\Phi_1$, and $V_4=\frac{1}{2}\Phi_2^T\Phi_2$. Then, it is clear that $V$ is positive definite and radially unbounded with respect to $\mathbf{E}_2=[(\mathbf{x}-\mathbf{x}_t^*)^T,\bar{\mathbf{y}}^T,\Phi_1^T,\Phi_2^T]^T$. Then

$$\dot{V}_1\overset{a.e.}{=}-k_1(\mathbf{x}-\mathbf{x}_t^*)^T\left([\nabla_i f_i(\mathbf{y}_i)]_{vec}+\delta(t)\left(\mathbf{x}-\mathbf{r}(t)\right)\right)-\left(\mathbf{x}-\mathbf{x}_t^*\right)^T\left(\dot{\mathbf{x}}_t^*-\dot{\mathbf{r}}(t)\right)+\delta(t)k_1(\mathbf{x}-\mathbf{x}_t^*)^T\bar{\Theta}+\left(\mathbf{x}-\mathbf{x}_t^*\right)^T\bar{\Upsilon}. \quad (40)$$

It follows from $\|\bar{\Theta}\|\leq\chi\|\Phi_1\|$ and $\|\bar{\Upsilon}\|\leq\chi\|\Phi_2\|$ that $\delta(t)(\mathbf{x}-\mathbf{x}_t^*)^T\bar{\Theta}\leq\delta(t)\|\mathbf{x}-\mathbf{x}_t^*\|\|\bar{\Theta}\|\leq\delta(t)\chi\|\mathbf{x}-\mathbf{x}_t^*\|\|\Phi_1\|$ and $(\mathbf{x}-\mathbf{x}_t^*)^T\bar{\Upsilon}\leq\|\mathbf{x}-\mathbf{x}_t^*\|\|\bar{\Upsilon}\|\leq\chi\|\mathbf{x}-\mathbf{x}_t^*\|\|\Phi_2\|$. Thus

$$\dot{V}_1\overset{a.e.}{\leq}-\delta(t)k_1\|\mathbf{x}-\mathbf{x}_t^*\|^2+\|\mathbf{x}-\mathbf{x}_t^*\|\|\dot{\mathbf{x}}_t^*-\dot{\mathbf{r}}(t)\|+\frac{3\delta(t)k_1}{8}\|\mathbf{x}-\mathbf{x}_t^*\|^2+\frac{2k_1(\max_{i\in\mathcal{N}}\{l_i\})^2}{\delta(t)}\|\bar{\mathbf{y}}\|^2+2\delta(t)\chi^2\|\Phi_1\|^2+\frac{2\chi^2}{\delta(t)k_1}\|\Phi_2\|^2. \quad (41)$$

Moreover, by Lemma 1, the time derivative of $V_2$ satisfies

$$\begin{aligned}\dot{V}_2&=\bar{\mathbf{y}}^T\mathcal{P}\left(-\omega(t)(\mathcal{L}\otimes I_{mN}+B_0)\bar{\mathbf{y}}-\mathbf{1}_N\otimes\dot{\mathbf{x}}+\mathbf{1}_N\otimes\Upsilon\right)\\&\quad+\left(-\omega(t)(\mathcal{L}\otimes I_{mN}+B_0)\bar{\mathbf{y}}-\mathbf{1}_N\otimes\dot{\mathbf{x}}+\mathbf{1}_N\otimes\Upsilon\right)^T\mathcal{P}\bar{\mathbf{y}}\\&=-\omega(t)\bar{\mathbf{y}}^T\mathcal{Q}\bar{\mathbf{y}}-2k_1\bar{\mathbf{y}}^T\mathcal{P}\left(\mathbf{1}_N\otimes\delta(t)\bar{\Theta}\right)\\&\quad+2k_1\bar{\mathbf{y}}^T\mathcal{P}\left(\mathbf{1}_N\otimes\left([\nabla_i f_i(\mathbf{y}_i)]_{vec}+\delta(t)\left(\mathbf{x}-\mathbf{r}(t)\right)\right)\right)\\&\leq-\lambda_{\min}(\mathcal{Q})\omega(t)\|\bar{\mathbf{y}}\|^2+2k_1\delta(t)\sqrt{N}\|\mathcal{P}\|\|\bar{\mathbf{y}}\|\|\bar{\Theta}\|\\&\quad+2k_1\sqrt{N}\|\mathcal{P}\|\left(\sqrt{N}\max_{i\in\mathcal{N}}\{l_i\}+\delta(t)\right)\|\bar{\mathbf{y}}\|\|\mathbf{x}-\mathbf{x}_t^*\|\\&\quad+2k_1\sqrt{N}\|\mathcal{P}\|\max_{i\in\mathcal{N}}\{l_i\}\|\bar{\mathbf{y}}\|^2\\&\leq-\left(\lambda_{\min}(\mathcal{Q})\omega(t)-2k_1\sqrt{N}\|\mathcal{P}\|\max_{i\in\mathcal{N}}\{l_i\}\right.\end{aligned}$$

$$-8k_1N\|\mathcal{P}\|^2(\sqrt{N}\max_{i\in\mathcal{N}}\{l_i\}+\delta(t))^2/\delta(t)-\delta(t)k_1\Big)$$
$$\times\|\bar{\mathbf{y}}\|^2+(\delta(t)k_1/8)\|\mathbf{x}-\mathbf{x}_t^*\|^2+\delta(t)k_1N\chi^2\|\mathcal{P}\|^2\|\Phi_1\|^2. \quad (42)$$

In addition

$$\dot{V}_3+\dot{V}_4=-\alpha(t)\|\Phi_1\|^2-\beta(t)\|\Phi_2\|^2. \quad (43)$$

Hence, it follows from (41)–(43) that:

$$\dot{V}\overset{a.e.}{\leq}-\frac{\delta(t)k_1}{2}\|\mathbf{x}-\mathbf{x}_t^*\|^2-\varrho_1(t)\|\bar{\mathbf{y}}\|^2-\varrho_2(t)\|\Phi_1\|^2$$
$$-\varrho_3(t)\|\Phi_2\|^2+\|\mathbf{x}-\mathbf{x}_t^*\|\|\dot{\mathbf{x}}_t^*-\dot{\mathbf{r}}(t)\| \quad (44)$$

where $\varrho_1(t)=\lambda_{\min}(\mathcal{Q})\omega(t)-\frac{2k_1(\max_{i\in\mathcal{N}}\{l_i\})^2}{\delta(t)}-2k_1\sqrt{N}\|\mathcal{P}\|\max_{i\in\mathcal{N}}\{l_i\}-\frac{8k_1N\|\mathcal{P}\|^2(\sqrt{N}\max_{i\in\mathcal{N}}\{l_i\}+\delta(t))^2}{\delta(t)}-\delta(t)k_1$, $\varrho_2(t)=\alpha(t)-2\delta(t)\chi^2-\delta(t)k_1N\chi^2\|\mathcal{P}\|^2$, and $\varrho_3(t)=\beta(t)-\frac{2\chi^2}{\delta(t)k_1}$. Choose $\omega(t)$, $\alpha(t)$ and $\beta(t)$ such that $\frac{\delta(t)k_1}{2}\leq\varrho_1(t)$, $\frac{\delta(t)k_1}{2}\leq\varrho_2(t)$, and $\frac{\delta(t)k_1}{2}\leq\varrho_3(t)$. Then, it can be derived that

$$\dot{V}\overset{a.e.}{\leq}-\frac{\delta(t)k_1}{2}\left(\|\mathbf{x}-\mathbf{x}_t^*\|^2+\|\bar{\mathbf{y}}\|^2+\|\Phi_1\|^2+\|\Phi_2\|^2\right)$$
$$+\|\mathbf{x}-\mathbf{x}_t^*\|\|\dot{\mathbf{x}}_t^*-\dot{\mathbf{r}}(t)\|. \quad (45)$$

The remaining proof follows that of Theorem 1 and thus, is omitted here. □

Theorem 2 illustrates that though only a subset of agents can get access to the trajectory information of the moving target, the least-distance formation tracking problem can still be solved by the control law (34)–(35).

This section addresses first-order integrator-type agents and in the following, second-order integrator-type agents are considered.

## B. Second-Order Integrator-Type Systems

In this section, the dynamics of agents are described by

$$\dot{x}_i(t)=v_i(t),\ \dot{v}_i(t)=u_i(t),\quad i\in\mathcal{N}. \quad (46)$$

In what follows, the case in which the trajectory information of the target is available to all agents is first addressed, followed by the case in which it is only available to a subset of agents. Besides, the following assumption needs to be satisfied in the subsequent analysis.

*Assumption 5:* The first three order time derivatives of $r(t)$, i.e., $\dot{r}(t)$, $\ddot{r}(t)$, and $\dddot{r}(t)$, exist.

***1) Trajectory of the Moving Target is Available to All the Agents:*** Suppose that $r(t)$, $\dot{r}(t)$, and $\ddot{r}(t)$ are available to all agents, one can design $u_i$ as

$$u_i=-k(t)(v_i-\dot{r}(t))$$
$$-k(t)k_1\left(\nabla_i f_i(\mathbf{y}_i)+\delta(t)\left(x_i-r(t)\right)\right)+\ddot{r}(t), \quad (47)$$

for $i\in\mathcal{N}$, where $k(t)$ is a time-varying, positive, and smooth parameter to be determined.

Furthermore, for each $i,j\in\mathcal{N}$, $y_{ij}$ is updated by

$$\dot{y}_{ij}=-\omega(t)\left(\sum_{k=1}^{N}a_{ik}(y_{ij}-y_{kj})+a_{ij}(y_{ij}-x_j)\right)+\dot{r}(t) \quad (48)$$

where $\omega(t)$ is a time-varying, positive, and smooth parameter to be determined.

Then, based on (46)–(48)

$$\begin{cases}\dot{\mathbf{x}}=\mathbf{v}\\ \dot{\mathbf{v}}=-k(t)\left(\mathbf{v}-\dot{\mathbf{r}}(t)\right)\\ \quad -k(t)k_1\left([\nabla_i f_i(\mathbf{y}_i)]_{vec}+\delta(t)\left(\mathbf{x}-\mathbf{r}(t)\right)\right)+\ddot{\mathbf{r}}(t)\\ \dot{\mathbf{y}}=-\omega(t)(\mathcal{L}\otimes I_{mN}+B_0)\bar{\mathbf{y}}+\mathbf{1}_N\otimes\dot{\mathbf{r}}(t)\end{cases} \quad (49)$$

where $\mathbf{v}=[v_1^T,v_2^T,\ldots,v_N^T]^T$.

For notational convenience, let $H=\begin{bmatrix}h_{11}&h_{12}&\cdots&h_{1N}\\h_{21}&h_{22}&\cdots&h_{2N}\\ \vdots&&\ddots&\\ h_{N1}&h_{N2}&\cdots&h_{NN}\end{bmatrix}$ and $h_{ij}\in\mathbb{R}^{1\times N}$. Moreover, $h_{ij}=0_N^T$, for $i\neq j$ and $h_{ii}=[-o_{i1},-o_{i2},\ldots,\sum_{j=1,j\neq i}^{N}o_{ij},\ldots,-o_{iN}]$. Moreover, defining $b=\|(H\otimes I_m)(\mathcal{L}\otimes I_{mN}+B_0)\|$. Let $\bar{\mathbf{v}}=\mathbf{v}+k_1([\nabla_i f_i(\mathbf{y}_i)]_{vec}+\delta(t)(\mathbf{x}-\mathbf{r}(t)))-\dot{\mathbf{r}}(t)$. Note that by the definition of $H$, it can be obtained that $(H\otimes I_m)(\mathbf{1}_N\otimes\dot{\mathbf{r}}(t))=\mathbf{0}_{mN}$. Thus, one has

$$\begin{cases}\dot{\bar{\mathbf{x}}}\overset{a.e.}{=}\mathbf{v}-\dot{\mathbf{r}}(t)-(\dot{\mathbf{x}}_t^*-\dot{\mathbf{r}}(t))\\ \dot{\bar{\mathbf{v}}}=-k(t)\bar{\mathbf{v}}-k_1\omega(t)(H\otimes I_m)(\mathcal{L}\otimes I_{mN}+B_0)\bar{\mathbf{y}}\\ \quad +k_1\delta(t)\left(\mathbf{v}-\dot{\mathbf{r}}(t)\right)+k_1\dot{\delta}(t)\left(\mathbf{x}-\mathbf{r}(t)\right)\\ \dot{\bar{\mathbf{y}}}=-\omega(t)(\mathcal{L}\otimes I_{mN}+B_0)\bar{\mathbf{y}}-\mathbf{1}_N\otimes(\mathbf{v}-\dot{\mathbf{r}}(t)).\end{cases} \quad (50)$$

The following theorem illustrates the effectiveness of the least-distance formation tracking protocol (47)–(48).

*Theorem 3:* Under Assumptions 1–2 and 5, $(\mathbf{x},\mathbf{v},\mathbf{y})$ is globally asymptotically convergent to $(\mathbf{x}^*(t),\dot{\mathbf{r}}(t),\mathbf{1}_N\otimes\mathbf{x}^*(t))$ given that

$$\lim_{t\to\infty}\delta(t)=0,\ \lim_{t\to\infty}\int_0^t\delta(s)\mathrm{d}s=\infty$$
$$\lim_{t\to\infty}\frac{|\dot{\delta}(t)|}{\delta(t)}=0,\ \lim_{t\to\infty}\frac{|\dot{\delta}(t)|}{\delta^2(t)}=0$$
$$\delta(t)\omega(t)\lambda_{\min}(\mathcal{Q})\geq\Lambda_1(\delta),\ \delta(t)k(t)\geq\Lambda_2(\delta,\omega), \quad (51)$$

where $\Lambda_1(\delta)=k_1(\max_{i\in\mathcal{N}}\{l_i\}+2\sqrt{N}\|\mathcal{P}\|(\sqrt{N}\max_{i\in\mathcal{N}}\{l_i\}+\delta(t)))^2+2k_1\sqrt{N}\|\mathcal{P}\|\delta(t)\sqrt{N}\max_{i\in\mathcal{N}}\{l_i\}+\frac{k_1}{2}+\frac{N\|P\|^2}{k_1}\delta(t)+\frac{\delta^2(t)k_1}{4}$, and $\Lambda_2(\delta,\omega)=k_1(\delta^2(t)+\delta(t))+\frac{1}{k_1}+\frac{k_1\delta^2(t)(\omega(t)b+\delta(t)\max_{i\in\mathcal{N}}\{l_i\})^2}{2}+k_1(\delta(t)(\sqrt{N}\max_{i\in\mathcal{N}}\{l_i\}+\delta(t))+|\dot{\delta}(t)|)^2+\frac{\delta^2(t)k_1}{4}$.

*Proof:* Define $V=V_1+V_2+V_3$, where $V_1=\frac{1}{2}(\mathbf{x}-\mathbf{x}_t^*)^T(\mathbf{x}-\mathbf{x}_t^*)$, $V_2=\frac{1}{2}\bar{\mathbf{v}}^T\bar{\mathbf{v}}$, and $V_3=\bar{\mathbf{y}}^T\mathcal{P}\bar{\mathbf{y}}$. Then, it is clear that $V$ is positive definite and radially unbounded with respect to $\mathbf{E}_3=[\bar{\mathbf{x}}^T,\bar{\mathbf{v}}^T,\bar{\mathbf{y}}^T]^T$. Therefore

$$\dot{V}_1\overset{a.e.}{=}(\mathbf{x}-\mathbf{x}_t^*)^T\bar{\mathbf{v}}-(\mathbf{x}-\mathbf{x}_t^*)^T\left(\dot{\mathbf{x}}_t^*-\dot{\mathbf{r}}(t)\right)$$
$$-k_1(\mathbf{x}-\mathbf{x}_t^*)^T\left([\nabla_i f_i(\mathbf{y}_i)]_{\text{vec}}+\delta(t)\left(\mathbf{x}-\mathbf{r}(t)\right)\right)$$
$$\overset{a.e.}{\leq}-\delta(t)k_1\|\mathbf{x}-\mathbf{x}_t^*\|^2+\|\mathbf{x}-\mathbf{x}_t^*\|\|\bar{\mathbf{v}}\|$$
$$+k_1\max_{i\in\mathcal{N}}\{l_i\}\|\mathbf{x}-\mathbf{x}_t^*\|\|\bar{\mathbf{y}}\|+\|\mathbf{x}-\mathbf{x}_t^*\|\|\dot{\mathbf{x}}_t^*-\dot{\mathbf{r}}(t)\|. \quad (52)$$

Moreover,

$$\dot{V}_2=-k(t)\|\bar{\mathbf{v}}\|^2-k_1\omega(t)\bar{\mathbf{v}}^T(H\otimes I_m)(\mathcal{L}\otimes I_{mN}+B_0)\bar{\mathbf{y}}$$
$$+k_1\delta(t)\|\bar{\mathbf{v}}\|^2-k_1\delta(t)\bar{\mathbf{v}}^T\left([\nabla_i f_i(\mathbf{y}_i)]_{\text{vec}}+\delta(t)\left(\mathbf{x}-\mathbf{r}(t)\right)\right)$$
$$+k_1\dot{\delta}(t)\bar{\mathbf{v}}^T(\mathbf{x}-\mathbf{x}_t^*)+k_1\dot{\delta}(t)\bar{\mathbf{v}}^T(\mathbf{x}_t^*-\mathbf{r}(t))$$
$$\leq-\left(k(t)-k_1\delta(t)\right)\|\bar{\mathbf{v}}\|^2+k_1\omega(t)b\|\bar{\mathbf{v}}\|\|\bar{\mathbf{y}}\|$$
$$+k_1\delta(t)\max_{i\in\mathcal{N}}\{l_i\}\|\bar{\mathbf{v}}\|\|\bar{\mathbf{y}}\|$$

$$+ k_1\delta(t)\left(\sqrt{N}\max_{i\in\mathcal{N}}\{l_i\}+\delta(t)\right)\|\bar{\mathbf{v}}\|\|\mathbf{x}-\mathbf{x}_t^*\|$$
$$+ k_1|\dot{\delta}(t)|\|\bar{\mathbf{v}}\|\|\mathbf{x}-\mathbf{x}_t^*\| + k_1|\dot{\delta}(t)|\|\bar{\mathbf{v}}\|\|\mathbf{x}_t^*-\mathbf{r}(t)\|. \quad (53)$$

In addition

$$\begin{aligned}\dot{V}_3 &= \bar{\mathbf{y}}^T\mathcal{P}\left(-\omega(t)(\mathcal{L}\otimes I_{mN}+B_0)\bar{\mathbf{y}}-\mathbf{1}_N\otimes(\mathbf{v}-\dot{\mathbf{r}}(t))\right)\\
&\quad+\left(-\omega(t)(\mathcal{L}\otimes I_{mN}+B_0)\bar{\mathbf{y}}-\mathbf{1}_N\otimes(\mathbf{v}-\dot{\mathbf{r}}(t))\right)^T\mathcal{P}\bar{\mathbf{y}}\\
&= -\omega(t)\bar{\mathbf{y}}^T\mathcal{Q}\bar{\mathbf{y}} - 2\bar{\mathbf{y}}^T\mathcal{P}\left(\mathbf{1}_N\otimes\bar{\mathbf{v}}\right)\\
&\quad+2k_1\bar{\mathbf{y}}^T\mathcal{P}\left(\mathbf{1}_N\otimes\left([\nabla_i f_i(\mathbf{y}_i)]_{\text{vec}}+\delta(t)\left(\mathbf{x}-\mathbf{r}(t)\right)\right)\right)\\
&\le -\left(\omega(t)\lambda_{\min}(\mathcal{Q})-2k_1\sqrt{N}\|\mathcal{P}\|\max_{i\in\mathcal{N}}\{l_i\}\right)\|\bar{\mathbf{y}}\|^2\\
&\quad+2k_1\sqrt{N}\|\mathcal{P}\|\left(\sqrt{N}\max_{i\in\mathcal{N}}\{l_i\}+\delta(t)\right)\|\bar{\mathbf{y}}\|\|\mathbf{x}-\mathbf{x}_t^*\|\\
&\quad+2\sqrt{N}\|\mathcal{P}\|\|\bar{\mathbf{v}}\|\|\bar{\mathbf{y}}\|. \end{aligned}\quad (54)$$

Hence, by (52)–(54), it can be obtained that

$$\begin{aligned}\dot{V} &\overset{a.e.}{\le} -\delta(t)k_1\|\mathbf{x}-\mathbf{x}_t^*\|^2-\left(k(t)-k_1\delta(t)\right)\|\bar{\mathbf{v}}\|^2\\
&\quad-\left(\omega(t)\lambda_{\min}(\mathcal{Q})-2k_1\sqrt{N}\|\mathcal{P}\|\max_{i\in\mathcal{N}}\{l_i\}\right)\|\bar{\mathbf{y}}\|^2\\
&\quad+k_1\left(\delta(t)\left(\sqrt{N}\max_{i\in\mathcal{N}}\{l_i\}+\delta(t)\right)+|\dot{\delta}(t)|\right)\\
&\qquad\times\|\mathbf{x}-\mathbf{x}_t^*\|\|\bar{\mathbf{v}}\|+\|\mathbf{x}-\mathbf{x}_t^*\|\|\bar{\mathbf{v}}\|\\
&\quad+k_1\left(\max_{i\in\mathcal{N}}\{l_i\}+2\sqrt{N}\|\mathcal{P}\|\right.\\
&\qquad\left.\times\left(\sqrt{N}\max_{i\in\mathcal{N}}\{l_i\}+\delta(t)\right)\right)\\
&\qquad\times\|\mathbf{x}-\mathbf{x}_t^*\|\|\bar{\mathbf{y}}\|+\|\mathbf{x}-\mathbf{x}_t^*\|\|\dot{\mathbf{x}}_t^*-\dot{\mathbf{r}}(t)\|\\
&\quad+k_1|\dot{\delta}(t)|\|\bar{\mathbf{v}}\|\|\mathbf{x}_t^*-\mathbf{r}(t)\|+2\sqrt{N}\|\mathcal{P}\|\|\bar{\mathbf{v}}\|\|\bar{\mathbf{y}}\|\\
&\quad+k_1\left(\omega(t)b+\delta(t)\max_{i\in\mathcal{N}}\{l_i\}\right)\|\bar{\mathbf{v}}\|\|\bar{\mathbf{y}}\|\\
&\overset{a.e.}{\le} -\frac{\delta(t)k_1}{4}\|\mathbf{x}-\mathbf{x}_t^*\|^2-\Psi_1(t)\|\bar{\mathbf{y}}\|^2-\Psi_2(t)\|\bar{\mathbf{v}}\|^2\\
&\quad+\|\mathbf{x}-\mathbf{x}_t^*\|\|\dot{\mathbf{x}}_t^*-\dot{\mathbf{r}}(t)\|+|\dot{\delta}(t)|\|\bar{\mathbf{v}}\|\|\mathbf{x}_t^*-\mathbf{r}(t)\| \end{aligned}\quad (55)$$

where $\Psi_1(t)=\omega(t)\lambda_{\min}(\mathcal{Q})-2k_1\sqrt{N}\|\mathcal{P}\|\max_{i\in\mathcal{N}}\{l_i\}-(k_1/2)-(N\|P\|^2/k_1)-k_1(\max_{i\in\mathcal{N}}\{l_i\}+2\sqrt{N}\|\mathcal{P}\|(\sqrt{N}\max_{i\in\mathcal{N}}\{l_i\}+\delta(t)))^2/\delta(t)$, $\Psi_2(t)=k(t)-(1/\delta(t)k_1)-k_1(\omega(t)b+\delta(t)\max_{i\in\mathcal{N}}\{l_i\})^2/2-k_1\delta(t)-k_1-k_1(\delta(t)(\sqrt{N}\max_{i\in\mathcal{N}}\{l_i\}+\delta(t))+|\dot{\delta}(t)|)^2/\delta(t)$. Choose $\omega(t)$ and $k(t)$ such that $\frac{\delta(t)k_1}{4}\le\Psi_1(t)$ and $\frac{\delta(t)k_1}{4}\le\Psi_2(t)$. Then, it can be derived that

$$\begin{aligned}\dot{V} &\overset{a.e.}{\le} -\frac{\delta(t)k_1}{4}\left(\|\mathbf{x}-\mathbf{x}_t^*\|^2+\|\bar{\mathbf{y}}\|^2+\|\bar{\mathbf{v}}\|^2\right)\\
&\quad+\|\mathbf{x}-\mathbf{x}_t^*\|\|\dot{\mathbf{x}}_t^*-\dot{\mathbf{r}}(t)\|+k_1|\dot{\delta}(t)|\|\bar{\mathbf{v}}\|\|\mathbf{x}_t^*-\mathbf{r}(t)\|. \end{aligned}\quad (56)$$

Recalling the definition of $V$, one has $\min\{\frac{1}{2},\lambda_{\min}(\mathcal{P})\}\|\mathbf{E}_3\|^2\le V\le\max\{\frac{1}{2},\lambda_{\max}(\mathcal{P})\}\|\mathbf{E}_3\|^2$. Therefore

$$\begin{aligned}\dot{V} &\overset{a.e.}{\le} -\frac{\delta(t)k_1}{4\max\{\frac{1}{2},\lambda_{\max}(\mathcal{P})\}}V\\
&\quad+\sqrt{2V}\left(\|\dot{\mathbf{x}}_t^*-\dot{\mathbf{r}}(t)\|+|\dot{\delta}(t)|\|\mathbf{x}_t^*-\mathbf{r}(t)\|\right). \end{aligned}\quad (57)$$

Let $J=\sqrt{2V}$ and $E(t)=\int_{s=0}^{t}\frac{\delta(s)k_1}{8\max\{\frac{1}{2},\lambda_{\max}(\mathcal{P})\}}\mathrm{d}s$. It follows from Corollary 1 that $\|\dot{\mathbf{x}}_t^*-\dot{\mathbf{r}}(t)\|\le c_x\frac{|\dot{\delta}(t)|}{\delta(t)}$ and $\|\mathbf{x}_t^*-\mathbf{r}(t)\|$ is bounded. Thus

$$\dot{J}\overset{a.e.}{\le}-\frac{\delta(t)k_1}{8\max\{\frac{1}{2},\lambda_{\max}(\mathcal{P})\}}J+c_x\frac{|\dot{\delta}(t)|}{\delta(t)}+C_p|\dot{\delta}(t)| \quad (58)$$

where $C_p\ge k_1\|\mathbf{x}_t^*-\mathbf{r}(t)\|$. Moreover

$$\frac{\mathrm{d}}{\mathrm{dt}}(Je^{E(t)})\overset{a.e.}{\le}\left(c_x\frac{|\dot{\delta}(t)|}{\delta(t)}+C_p|\dot{\delta}(t)|\right)e^{E(t)}. \quad (59)$$

Taking integration on both sides of (59) over $[0,T]$, it can be derived that

$$J(T)e^{E(T)}-J(0)\le\int_0^T\left(c_x\frac{|\dot{\delta}(s)|}{\delta(s)}+C_p|\dot{\delta}(s)|\right)e^{E(s)}\mathrm{d}s \quad (60)$$

and hence

$$\begin{aligned}0&\le J(T)\le e^{-E(T)}J(0)\\
&\quad+e^{-E(T)}\int_0^T\left(c_x\frac{|\dot{\delta}(s)|}{\delta(s)}+C_p|\dot{\delta}(s)|\right)e^{E(s)}\mathrm{d}s. \end{aligned}\quad (61)$$

Since $\lim_{t\to\infty}\int_0^t\delta(s)\mathrm{d}s=\infty$, $\lim_{t\to\infty}e^{-E(t)}=0$. In addition, as $\lim_{t\to\infty}\frac{|\dot{\delta}(t)|}{\delta^2(t)}=0$, one has $\lim_{t\to\infty}e^{-E(t)}\int_0^t c_x\frac{|\dot{\delta}(s)|}{\delta(s)}e^{E(s)}\mathrm{d}s=0$. Similarly, as $\lim_{t\to\infty}\frac{|\dot{\delta}(t)|}{\delta(t)}=0$, it can be derived that $\lim_{t\to\infty}e^{-E(t)}\int_0^t C_p|\dot{\delta}(s)|e^{E(s)}\mathrm{d}s=0$. Then, it is clear that $\lim_{t\to\infty}J(t)=0$.

Thus, $\lim_{t\to\infty}\|\mathbf{x}(t)-\mathbf{x}_t^*\|=0$, $\lim_{t\to\infty}\|\bar{\mathbf{v}}(t)\|=0$ and $\lim_{t\to\infty}\|\bar{\mathbf{y}}(t)\|=0$. Furthermore, it results from $F(\mathbf{x}_t^*)+\delta(t)(\mathbf{x}_t^*-\mathbf{r}(t))=\mathbf{0}_{mN}$ that $\lim_{t\to\infty}\|\mathbf{v}(t)-\dot{\mathbf{r}}(t)\|=0$. Moreover, by Corollary 1, $\lim_{t\to\infty}(\mathbf{x}_t^*-\mathbf{x}^*(t))=\mathbf{0}_{mN}$, which further indicates that $\lim_{t\to\infty}\|\mathbf{x}(t)-\mathbf{x}^*(t)\|=0$, and $\lim_{t\to\infty}\|\mathbf{y}(t)-\mathbf{1}_N\otimes\mathbf{x}^*(t)\|=0$. Hence, the conclusion is derived.

Theorem 3 demonstrates that with the trajectory information of the moving target known to all agents, protocol (47)–(48) can be employed to solve the least- distance formation tracking problem. It is worth mentioning that by the modular framework [38], one can also design the least-distance formation tracking protocol as

$$\begin{cases}\dot{x}_i=v_i\\ \dot{v}_i=-(x_i-z_i)-(v_i-\dot{r}(t))+\ddot{r}(t)\\ \dot{z}_i=-k_1\left(\nabla_i f_i(\mathbf{y}_i)+\delta(t)\left(z_i-r(t)\right)\right)+\dot{r}(t)\end{cases} \quad (62)$$

for $i\in\mathcal{N}$, where $z_i\in\mathbb{R}^m$ is an auxiliary vector. Furthermore, for each $i,j\in\mathcal{N}$, $y_{ij}$ is updated by

$$\dot{y}_{ij}=-\omega(t)\left(\sum_{k=1}^{N}a_{ik}(y_{ij}-y_{kj})+a_{ij}(y_{ij}-z_j)\right)+\dot{r}(t). \quad (63)$$

Define $\mathbf{z}=[z_1^T,z_2^T,\ldots,z_N^T]^T$. Then, the following corollary can be obtained for (62)–(63).

*Corollary 3:* Under Assumptions 1-2 and 5, $(\mathbf{x},\mathbf{z},\mathbf{v},\mathbf{y})$ is globally asymptotically convergent to $(\mathbf{x}^*(t),\mathbf{x}^*(t),\dot{\mathbf{r}}(t),\mathbf{1}_N\otimes\mathbf{x}^*(t))$, if $\delta(t)$ and $\omega(t)$ are chosen to satisfy (17).

*Proof:* Define $\tilde{x}_i = x_i - z_i$ and $\tilde{v}_i = v_i - \dot{r}(t)$. By (62), it can be derived that

$$\begin{bmatrix}\dot{\tilde{x}}_i \\ \dot{\tilde{v}}_i\end{bmatrix} = \begin{bmatrix}0 & 1 \\ -1 & -1\end{bmatrix}\begin{bmatrix}\tilde{x}_i \\ \tilde{v}_i\end{bmatrix} + \begin{bmatrix}-(\dot{z}_i - \dot{r}(t)) \\ 0\end{bmatrix}. \quad (64)$$

Since $\begin{bmatrix}0 & 1 \\ -1 & -1\end{bmatrix}$ is Hurwitz, it is clear that (64) is input-to-state stable if $\dot{z}_i - \dot{r}(t)$ is viewed as the virtual control input.

Then, by Theorem 1, it can be obtained that $\lim_{t\to\infty}(\mathbf{y}_i(t) - \mathbf{x}_t^*) = \mathbf{0}_{mN}$, $\lim_{t\to\infty}(\mathbf{z}(t) - \mathbf{x}_t^*) = \mathbf{0}_{mN}$ and $\lim_{t\to\infty}\delta(t) = 0$. Therefore

$$\lim_{t\to\infty}(\dot{z}_i(t) - \dot{r}(t)) = \mathbf{0}_m \quad (65)$$

which implies that $\lim_{t\to\infty}\tilde{x}_i(t) = \mathbf{0}_m$ and $\lim_{t\to\infty}\tilde{v}_i(t) = \mathbf{0}_m$, thus arriving at the conclusion. □

If $o_{ij} = a_{ij}$ and $r(t), \dot{r}(t), \ddot{r}(t)$ are available to all agents, $u_i$ can be designed as

$$\begin{aligned} u_i = & -k(t)(v_i - \dot{r}(t)) \\ & -k(t)k_1\Big(\nabla_i f_i(\mathbf{x}) + \delta(t)(x_i - r(t))\Big) + \ddot{r}(t) \end{aligned} \quad (66)$$

for $i \in \mathcal{N}$, where $k(t)$ is a time-varying, positive, and smooth parameter. Then, the following corollary can be obtained.

*Corollary 4:* Suppose that Assumptions 1 and 5 hold and the graph $\mathcal{G}$ is weight-balanced

$$\lim_{t\to\infty}\|\mathbf{x}(t) - \mathbf{x}^*(t)\| = 0, \quad \lim_{t\to\infty}\|\mathbf{v}(t) - \dot{\mathbf{r}}(t)\| = 0 \quad (67)$$

if $\delta(t)$ and $k(t)$ are chosen such that $\lim_{t\to\infty}\delta(t) = 0$, $\lim_{t\to\infty}\int_0^t \delta(s)ds = \infty$, $\lim_{t\to\infty}\frac{|\dot{\delta}(t)|}{\delta^2(t)} = 0$, and $\delta(t)k(t) \geq \bar{c}(\delta)$, where $\bar{c}(\delta) = \frac{\delta^2(t)k_1}{2} + k_1\delta^2(t) + hk_1\delta(t) + k_1((\delta(t) + h)(\sqrt{N}\max_{i\in\mathcal{N}}\{l_i\} + \delta(t)) + |\dot{\delta}(t)| + 1)^2/2 + (1/k_1)$ and $h = \|\Omega \otimes I_m\|$.

*Proof:* Define $V_1 = \frac{1}{2}(\mathbf{x} - \mathbf{x}_t^*)^T(\mathbf{x} - \mathbf{x}_t^*)$ and $V_2 = \frac{1}{2}\hat{\mathbf{v}}^T\hat{\mathbf{v}}$, where $\hat{\mathbf{v}} = \mathbf{v} + k_1(F(\mathbf{x}) + \delta(t)(\mathbf{x} - \mathbf{r}(t))) - \dot{\mathbf{r}}(t)$. Let $V = V_1 + V_2$, then, it is clear that $V$ is positive definite and radially unbounded with respect to $\mathbf{E}_4 = [(\mathbf{x} - \mathbf{x}_t^*)^T, \hat{\mathbf{v}}^T]^T$. Then

$$\begin{aligned} \dot{V}_1 \leq & -\delta(t)k_1\|\mathbf{x} - \mathbf{x}_t^*\|^2 + \|\mathbf{x} - \mathbf{x}_t^*\|\|\hat{\mathbf{v}}\| \\ & + \|\mathbf{x} - \mathbf{x}_t^*\|\|\dot{\mathbf{x}}_t^* - \dot{\mathbf{r}}(t)\|. \end{aligned} \quad (68)$$

Moreover, since $\dot{\hat{\mathbf{v}}} = -k(t)\hat{\mathbf{v}} + k_1(\Omega \otimes I_m)\hat{\mathbf{v}} - k_1(\Omega \otimes I_m)(F(\mathbf{x}) + \delta(t)(\mathbf{x} - \mathbf{r}(t))) + k_1\delta(t)\hat{\mathbf{v}} - k_1\delta(t)(F(\mathbf{x}) + \delta(t)(\mathbf{x} - \mathbf{r}(t))) + k_1\dot{\delta}(t)(\mathbf{x} - \mathbf{r}(t))$, one has

$$\begin{aligned} \dot{V}_2 = \hat{\mathbf{v}}^T\dot{\hat{\mathbf{v}}} \leq & -(k(t) - hk_1 - \delta(t)k_1)\|\hat{\mathbf{v}}\|^2 \\ & + k_1(h + \delta(t))(\delta(t) + \sqrt{N}\max_{i\in\mathcal{N}}\{l_i\})\|\hat{\mathbf{v}}\|\|\mathbf{x} - \mathbf{x}_t^*\| \\ & + k_1|\dot{\delta}(t)|\|\hat{\mathbf{v}}\|\|\mathbf{x} - \mathbf{x}_t^*\| + k_1|\dot{\delta}(t)|\|\hat{\mathbf{v}}\|\|\mathbf{x}_t^* - \mathbf{r}(t)\|. \end{aligned} \quad (69)$$

Hence, by (68) and (69), one has

$$\begin{aligned} \dot{V} \overset{a.e.}{\leq} & -\frac{\delta(t)k_1}{2}\|\mathbf{x} - \mathbf{x}_t^*\|^2 - \bar{\epsilon}(t)\|\hat{\mathbf{v}}\|^2 \\ & + k_1|\dot{\delta}(t)|\|\hat{\mathbf{v}}\|\|\mathbf{x}_t^* - \mathbf{r}(t)\| + \|\mathbf{x} - \mathbf{x}_t^*\|\|\dot{\mathbf{x}}_t^* - \dot{\mathbf{r}}(t)\| \end{aligned} \quad (70)$$

where $\bar{\epsilon}(t) = k(t) - hk_1 - \delta(t)k_1 - k_1((\delta(t) + h)(\delta(t) + \sqrt{N}\max_{i\in\mathcal{N}}\{l_i\}) + |\dot{\delta}(t)| + 1)^2/(\delta(t)) - (1/\delta(t)k_1)$. Choosing $k(t)$ to be sufficiently large such that $\frac{\delta(t)k_1}{2} \leq \bar{\epsilon}(t)$, one has

$$\begin{aligned} \dot{V} \overset{a.e.}{\leq} & -\frac{\delta(t)k_1}{2}\|\mathbf{E}_4\|^2 + \|\mathbf{x} - \mathbf{x}_t^*\|\|\dot{\mathbf{x}}_t^* - \dot{\mathbf{r}}(t)\| \\ & + k_1|\dot{\delta}(t)|\|\hat{\mathbf{v}}\|\|\mathbf{x}_t^* - \mathbf{r}(t)\|. \end{aligned} \quad (71)$$

The remaining analysis follows that proof of Theorem 3 and hence, is omitted here. □

*Remark 8:* Corollaries 2 and 4 show that by setting $o_{ij} = a_{ij}$, there is no need to have a local estimate on other agents' positions, thus relaxing the communication burden. However, the communication graph is required to be weight-balanced in this case, which is a sacrifice to align the interference graph with the communication graph. That is to say, by allowing $o_{ij}$ to be different from $a_{ij}$, we accommodate unbalanced digraphs while covering more general games.

In the following, the case in which the trajectory information of the moving target is only available to a subset of agents is further considered.

### 2) Trajectory of the Moving Target is Available to a Subset of the Agents:

With $r(t)$, $\dot{r}(t)$, and $\ddot{r}(t)$ available to only a subset of agents, the control input $u_i$ can be designed as

$$\begin{cases} u_i = -k(t)(v_i - \gamma_i(t)) \\ \qquad -k(t)k_1(\nabla_i f_i(\mathbf{y}_i) + \delta(t)(x_i - \theta_i(t))) + \varpi_i(t) \\ \dot{y}_{ij} = -\omega(t)(a_{ik}(y_{ij} - y_{kj}) + a_{ij}(y_{ij} - x_j)) + \gamma_i(t) \end{cases} \quad (72)$$

for $i, j \in \mathcal{N}$, where $\theta_i(t) \in \mathbb{R}^m$, $\gamma_i(t) \in \mathbb{R}^m$, and $\varpi_i(t) \in \mathbb{R}^m$ are the estimates of $r(t)$, $\dot{r}(t)$, and $\ddot{r}(t)$, respectively.

Let $\mathbf{q}_i = [\theta_i^T(t), \gamma_i^T(t), \varpi_i^T(t)]^T$, $\tilde{\mathbf{r}}_2 = [r(t)^T, \dot{r}(t)^T, \ddot{r}(t)^T]^T$, and $\varphi_2(t) = \mathrm{diag}\{\alpha(t), \beta(t), \iota(t)\} \otimes I_m$, where $\alpha(t)$, $\beta(t)$, and $\iota(t)$ are time-varying, positive, and smooth parameters. Then, for each $i \in \mathcal{N}$, $\mathbf{q}_i$ is generated by

$$\begin{aligned} \dot{\mathbf{q}}_i = & \frac{1}{\sum_{j=1}^N a_{ij} + \eta_i}\sum_{j=1}^N a_{ij}(\dot{\mathbf{q}}_j - \varphi_2(t)(\mathbf{q}_i - \mathbf{q}_j)) \\ & + \frac{\eta_i}{\sum_{j=1}^N a_{ij} + \eta_i}\Big(\dot{\tilde{\mathbf{r}}}_2 - \varphi_2(t)(\mathbf{q}_i - \tilde{\mathbf{r}}_2)\Big) \end{aligned} \quad (73)$$

where $\eta_i = 1$ indicates that agent $i$ can receive the information of the moving target (e.g., $r(t)$, $\dot{r}(t)$, and $\ddot{r}(t)$), and vice versa, $\eta_i = 0$.

By (46) and (72), one can get that

$$\begin{cases} \dot{\mathbf{x}} = \mathbf{v} \\ \dot{\mathbf{v}} = -k(t)(\mathbf{v} - \Upsilon) - k(t)k_1([\nabla_i f_i(\mathbf{y}_i)]_{vec} \\ \qquad + \delta(t)(\mathbf{x} - \Theta)) + \Pi \\ \dot{\mathbf{y}} = -\omega(t)(\mathcal{L} \otimes I_{mN} + B_0)\bar{\mathbf{y}} + \mathbf{1}_N \otimes \Upsilon \end{cases} \quad (74)$$

where $\Theta = [\theta_1^T, \theta_2^T, \ldots, \theta_N^T]^T$, $\Upsilon = [\gamma_1^T, \gamma_2^T, \ldots, \gamma_N^T]^T$ and $\Pi = [\varpi_1^T, \varpi_2^T, \ldots, \varpi_N^T]^T$.

Let $\bar{\Theta} = \Theta(t) - \mathbf{r}(t)$, $\bar{\Upsilon} = \Upsilon(t) - \dot{\mathbf{r}}(t)$ and $\bar{\Pi} = \Pi(t) - \ddot{\mathbf{r}}(t)$. Since $(H \otimes I_m)(\mathbf{1}_N \otimes \Upsilon) = \mathbf{0}_{mN}$, one has

$$\begin{cases} \dot{\bar{\mathbf{x}}} \overset{a.e.}{=} \mathbf{v} - \dot{\mathbf{r}}(t) - (\dot{\mathbf{x}}_t^* - \dot{\mathbf{r}}(t)) \\ \dot{\bar{\mathbf{v}}} = -k(t)\bar{\mathbf{v}} - k_1\omega(t)(H \otimes I_m)(\mathcal{L} \otimes I_{mN} + B_0)\bar{\mathbf{y}} \\ \qquad + k(t)\bar{\Upsilon} + k(t)k_1\delta(t)\bar{\Theta} + \delta(t)k_1(\mathbf{v} - \dot{\mathbf{r}}(t)) \\ \qquad + \dot{\delta}(t)k_1(\mathbf{x} - \mathbf{r}(t)) + \bar{\Pi} \\ \dot{\bar{\mathbf{y}}} = -\omega(t)(\mathcal{L} \otimes I_{mN} + B_0)\bar{\mathbf{y}} - \mathbf{1}_N \otimes \dot{\mathbf{x}} + \mathbf{1}_N \otimes \Upsilon. \end{cases} \quad (75)$$

Moreover, multiplying both sides of (73) by $\sum_{i=1}^j a_{ij} + \eta_i$ gives $(\sum_{i=1}^j a_{ij} + \eta_i)\dot{\mathbf{q}}_i = \sum_{j=1}^N a_{ij}(\dot{\mathbf{q}}_i - \varphi_2(t)(\mathbf{q}_i - \mathbf{q}_j)) + \eta_i(\dot{\tilde{\mathbf{r}}}_2 - \varphi_2(t)(\mathbf{q}_i - \tilde{\mathbf{r}}_2))$. Hence

$$(\mathcal{L} \otimes I_m + \Xi)(\dot{\Theta} - \dot{\mathbf{r}}) = -\alpha(t)(\mathcal{L} \otimes I_m + \Xi)(\Theta - \mathbf{r})$$

$$(\mathcal{L} \otimes I_m + \Xi)(\dot{\Upsilon} - \ddot{\mathbf{r}}) = -\beta(t)(\mathcal{L} \otimes I_m + \Xi)(\Theta - \dot{\mathbf{r}})$$

$$(\mathcal{L} \otimes I_m + \Xi)(\dot{\Pi} - \dddot{\mathbf{r}}) = -\iota(t)(\mathcal{L} \otimes I_m + \Xi)(\Pi - \ddot{\mathbf{r}})$$

where $\Xi = \mathrm{diag}\{\eta_i\}_{i\in\mathcal{N}} \otimes I_m$.

Defining $\Phi_1 = (\mathcal{L}\otimes I_m + \Xi)\bar{\Theta}$, $\Phi_2 = (\mathcal{L}\otimes I_m + \Xi)\bar{\Upsilon}$, and $\Phi_3 = (\mathcal{L}\otimes I_m + \Xi)\bar{\Pi}$. Then

$$\dot{\Phi}_1 = -\alpha(t)\Phi_1, \quad \dot{\Phi}_2 = -\beta(t)\Phi_2, \quad \dot{\Phi}_3 = -\iota(t)\Phi_3. \tag{76}$$

The following result can be derived for the least-distance formation tracking protocol in (72)–(73).

*Theorem 4:* Under Assumptions 1–2 and 4–5, $(\mathbf{x},\mathbf{v},\mathbf{y},\Theta,\Upsilon,\Pi)$ is globally asymptotically convergent to $(\mathbf{x}^*(t),\dot{\mathbf{r}}(t),\mathbf{1}_N\otimes\mathbf{x}^*(t),\mathbf{r}(t),\dot{\mathbf{r}}(t),\ddot{\mathbf{r}}(t))$ given that

$$\lim_{t\to\infty}\delta(t)=0, \lim_{t\to\infty}\int_0^t \delta(s)\mathrm{d}s=\infty, \lim_{t\to\infty}\frac{|\dot{\delta}(t)|}{\delta(t)}=0$$

$$\lim_{t\to\infty}\frac{|\dot{\delta}(t)|}{\delta^2(t)}=0, \delta(t)\omega(t)\lambda_{\min}(\mathcal{Q})\geq\Delta_1(\delta),$$

$$\delta(t)k(t)/4\geq\Delta_2(\delta,\omega)$$

$$\delta(t)\alpha(t)\geq\Delta_3(\delta,k), \delta(t)\beta(t)\geq\Delta_4(\delta,k), \delta(t)\iota(t)\geq\Delta_5(\delta)$$

where $\Delta_1(\delta) = k_1(\max_{i\in\mathcal{N}}\{l_i\} + 2\sqrt{N}\|\mathcal{P}\|(\sqrt{N}\max_{i\in\mathcal{N}}\{l_i\} + \delta(t)))^2 + 2\delta(t)k_1\sqrt{N}\|\mathcal{P}\|\max_{i\in\mathcal{N}}\{l_i\} + (\frac{k_1}{2} + \frac{N\|P\|^2}{k_1} + 1)\delta(t) + \frac{\delta^2(t)k_1}{4}$, $\Delta_2(\delta,\omega) = k_1(\delta(t)(\sqrt{N}\max_{i\in\mathcal{N}}\{l_i\} + \delta(t)) + |\dot{\delta}(t)|)^2 + k_1\delta(t)(\omega(t)b + \delta(t)\max_{i\in\mathcal{N}}\{l_i\})^2 + k_1\delta(t) + \frac{1}{k_1} + \frac{7k_1}{4}\delta^2(t)$, $\Delta_3(\delta,k) = k(t)k_1^2\delta^3(t)\chi^2 + \frac{\delta^2(t)k_1}{4}$, $\Delta_4(\delta,k) = N\delta(t)\|\mathcal{P}\|^2\chi^2 + \frac{\delta(t)k(t)\chi^2}{2} + \frac{\delta^2(t)k_1}{4}$, and $\Delta_5(\delta) = \frac{\chi^2}{2k_1} + \frac{\delta^2(t)k_1}{4}$.

*Proof:* Define $V = V_1+V_2+V_3+V_4+V_5+V_6$, where $V_1 = \frac{1}{2}(\mathbf{x}-\mathbf{x}_t^*)^T(\mathbf{x}-\mathbf{x}_t^*)$, $V_2 = \frac{1}{2}\bar{\mathbf{v}}^T\bar{\mathbf{v}}$, $V_3 = \bar{\mathbf{y}}^T\mathcal{P}\bar{\mathbf{y}}$, $V_4 = \frac{1}{2}\Phi_1^T\Phi_1$, $V_5 = \frac{1}{2}\Phi_2^T\Phi_2$, and $V_6 = \frac{1}{2}\Phi_3^T\Phi_3$. Then, it is clear that $V$ is positive definite and radially unbounded with respect to $\mathbf{E}_5 = [(\mathbf{x}-\mathbf{x}_t^*)^T,\bar{\mathbf{v}}^T,\bar{\mathbf{y}}^T,\Phi_1^T,\Phi_2^T,\Phi_3^T]^T$. Then

$$\begin{aligned}\dot{V}_1 \overset{a.e.}{\leq} &-\delta(t)k_1\|\mathbf{x}-\mathbf{x}_t^*\|^2 + \|\mathbf{x}-\mathbf{x}_t^*\|\|\bar{\mathbf{v}}\|\\ &+k_1\max_{i\in\mathcal{N}}\{l_i\}\|\mathbf{x}-\mathbf{x}_t^*\|\|\bar{\mathbf{y}}\| + \|\mathbf{x}-\mathbf{x}_t^*\|\|\dot{\mathbf{x}}_t^*-\dot{\mathbf{r}}(t)\|.\end{aligned} \tag{77}$$

Moreover

$$\begin{aligned}\dot{V}_2 = &-k(t)\|\bar{\mathbf{v}}\|^2 - k_1\omega(t)\bar{\mathbf{v}}^T(H\otimes I_m)(\mathcal{L}\otimes I_{mN}+B_0)\bar{\mathbf{y}}\\ &+k(t)\bar{\mathbf{v}}^T\bar{\Upsilon} + k(t)k_1\delta(t)\bar{\mathbf{v}}^T\bar{\Theta} + \bar{\mathbf{v}}^T\bar{\Pi}\\ &+\delta(t)k_1\|\bar{\mathbf{v}}\|^2 - \delta(t)k_1\bar{\mathbf{v}}^T([\nabla_i f_i(\mathbf{y}_i)]_{\mathrm{vec}}\\ &+\delta(t)(\mathbf{x}-\mathbf{r}(t)))\\ &+k_1\dot{\delta}(t)\bar{\mathbf{v}}^T(\mathbf{x}-\mathbf{x}_t^*) + k_1\dot{\delta}(t)\bar{\mathbf{v}}^T(\mathbf{x}_t^*-\mathbf{r}(t)).\end{aligned} \tag{78}$$

As $\bar{\mathbf{v}}^T\bar{\Theta}\leq\|\bar{\mathbf{v}}\|\|\bar{\Theta}\|$, $\bar{\mathbf{v}}^T\bar{\Upsilon}\leq\|\bar{\mathbf{v}}\|\|\bar{\Upsilon}\|$ and $\bar{\mathbf{v}}^T\bar{\Pi}\leq\|\bar{\mathbf{v}}\|\|\bar{\Pi}\|$, one has $\bar{\mathbf{v}}^T\bar{\Theta}\leq\chi\|\bar{\mathbf{v}}\|\|\Phi_1\|$, $\bar{\mathbf{v}}^T\bar{\Upsilon}\leq\chi\|\bar{\mathbf{v}}\|\|\Phi_2\|$, and $\bar{\mathbf{v}}^T\bar{\Pi}\leq\chi\|\bar{\mathbf{v}}\|\|\Phi_3\|$. In addition, noticing that $F(\mathbf{x}_t^*)+\delta(t)(\mathbf{x}_t^*-\mathbf{r}(t)) = \mathbf{0}_{mN}$, it can be derived that $\bar{\mathbf{v}}^T([\nabla_i f_i(\mathbf{y}_i)]_{\mathrm{vec}} + \delta(t)(\mathbf{x}-\mathbf{r}(t))) = \bar{\mathbf{v}}^T([\nabla_i f_i(\mathbf{y}_i)]_{\mathrm{vec}} + \delta(t)(\mathbf{x}-\mathbf{r}(t)) - F(\mathbf{x}) + F(\mathbf{x}) - F(\mathbf{x}_t^*) - \delta(t)(\mathbf{x}_t^*-\mathbf{r}(t)))\leq\max_{i\in\mathcal{N}}\{l_i\}\|\bar{\mathbf{v}}\|\|\bar{\mathbf{y}}\| + (\sqrt{N}\max_{i\in\mathcal{N}}\{l_i\}+\delta(t))\|\bar{\mathbf{v}}\|\|\mathbf{x}-\mathbf{x}_t^*\|$. Thus

$$\begin{aligned}\dot{V}_2 \leq &-(k(t)-\delta(t)k_1)\|\bar{\mathbf{v}}\|^2 + k_1\omega(t)b\|\bar{\mathbf{v}}\|\|\bar{\mathbf{y}}\|\\ &+k(t)k_1\delta(t)\chi\|\bar{\mathbf{v}}\|\|\Phi_1\| + k(t)\chi\|\bar{\mathbf{v}}\|\|\Phi_2\|\\ &+\chi\|\bar{\mathbf{v}}\|\|\Phi_3\| + \delta(t)k_1\max_{i\in\mathcal{N}}\{l_i\}\|\bar{\mathbf{v}}\|\|\bar{\mathbf{y}}\|\\ &+\delta(t)k_1\left(\sqrt{N}\max_{i\in\mathcal{N}}\{l_i\}+\delta(t)\right)\|\bar{\mathbf{v}}\|\|\mathbf{x}-\mathbf{x}_t^*\|\\ &+k_1|\dot{\delta}(t)|\|\bar{\mathbf{v}}\|\|\mathbf{x}-\mathbf{x}_t^*\| + k_1|\dot{\delta}(t)|\|\bar{\mathbf{v}}\|\|\mathbf{x}_t^*-\mathbf{r}(t)\|.\end{aligned} \tag{79}$$

In addition, by Lemma 1

$$\dot{V}_3 \leq -\omega(t)\lambda_{\min}(\mathcal{Q})\|\bar{\mathbf{y}}\|^2 - 2\bar{\mathbf{y}}^T\mathcal{P}(\mathbf{1}_N\otimes\dot{\mathbf{x}} - \mathbf{1}_N\otimes\Upsilon). \tag{80}$$

By (74), $-2\bar{\mathbf{y}}^T\mathcal{P}(\mathbf{1}_N\otimes\dot{\mathbf{x}}-\mathbf{1}_N\otimes\Upsilon) = -2\bar{\mathbf{y}}^T\mathcal{P}(\mathbf{1}_N\otimes\bar{\mathbf{v}} - \mathbf{1}_N\otimes k_1[([\nabla_i f_i(\mathbf{y}_i)]_{vec}+\delta(t)(\mathbf{x}-\mathbf{r}(t)))]-\mathbf{1}_N\otimes\bar{\Upsilon})\leq 2\sqrt{N}\|\mathcal{P}\|\|\bar{\mathbf{y}}\|\|\bar{\mathbf{v}}\| + 2k_1\sqrt{N}\|\mathcal{P}\|\max_{i\in\mathcal{N}}\{l_i\}\|\bar{\mathbf{y}}\|^2 + 2k_1\sqrt{N}\|\mathcal{P}\|(\sqrt{N}\max_{i\in\mathcal{N}}\{l_i\}+\delta(t))\|\bar{\mathbf{y}}\|\|\mathbf{x}-\mathbf{x}_t^*\| + 2\sqrt{N}\|\mathcal{P}\|\chi\|\bar{\mathbf{y}}\|\|\Phi_2\|$. Thus

$$\begin{aligned}\dot{V}_3 \leq &-(\omega(t)\lambda_{\min}(\mathcal{Q}) - 2k_1\sqrt{N}\|\mathcal{P}\|\max_{i\in\mathcal{N}}\{l_i\})\|\bar{\mathbf{y}}\|^2\\ &+2\sqrt{N}\|\mathcal{P}\|\|\bar{\mathbf{y}}\|\|\bar{\mathbf{v}}\| + 2\sqrt{N}\|\mathcal{P}\|\chi\|\bar{\mathbf{y}}\|\|\Phi_2\|\\ &+2k_1\sqrt{N}\|\mathcal{P}\|\left(\sqrt{N}\max_{i\in\mathcal{N}}\{l_i\}+\delta(t)\right)\|\bar{\mathbf{y}}\|\|\mathbf{x}-\mathbf{x}_t^*\|.\end{aligned} \tag{81}$$

Besides

$$\dot{V}_4+\dot{V}_5+\dot{V}_6 = -\alpha(t)\|\Phi_1\|^2 - \beta(t)\|\Phi_2\|^2 - \iota(t)\|\Phi_3\|^2. \tag{82}$$

Hence, by (77)–(82), one has

$$\begin{aligned}\dot{V} \overset{a.e.}{\leq} &-\delta(t)k_1\|\mathbf{x}-\mathbf{x}_t^*\|^2 - (k(t)-\delta(t)k_1)\|\bar{\mathbf{v}}\|^2\\ &-\left(\omega(t)\lambda_{\min}(\mathcal{Q}) - 2k_1\sqrt{N}\|\mathcal{P}\|\max_{i\in\mathcal{N}}\{l_i\}\right)\|\bar{\mathbf{y}}\|^2\\ &-\alpha(t)\|\Phi_1\|^2 - \beta(t)\|\Phi_2\|^2 - \iota(t)\|\Phi_3\|^2 + \|\mathbf{x}-\mathbf{x}_t^*\|\|\bar{\mathbf{v}}\|\\ &+k_1\left(\delta(t)\left(\sqrt{N}\max_{i\in\mathcal{N}}\{l_i\}+\delta(t)\right)+|\dot{\delta}(t)|\right)\|\mathbf{x}-\mathbf{x}_t^*\|\|\bar{\mathbf{v}}\|\\ &+k_1\left(\max_{i\in\mathcal{N}}\{l_i\}+2\sqrt{N}\|\mathcal{P}\|\left(\sqrt{N}\max_{i\in\mathcal{N}}\{l_i\}+\delta(t)\right)\right)\\ &\times\|\mathbf{x}-\mathbf{x}_t^*\|\|\bar{\mathbf{y}}\| + 2\sqrt{N}\|\mathcal{P}\|\chi\|\bar{\mathbf{y}}\|\|\Phi_2\| + 2\sqrt{N}\|\mathcal{P}\|\|\bar{\mathbf{v}}\|\|\bar{\mathbf{y}}\|\\ &+k_1(\omega(t)b+\delta(t)\max_{i\in\mathcal{N}}\{l_i\})\|\bar{\mathbf{v}}\|\|\bar{\mathbf{y}}\|\\ &+k(t)\delta(t)k_1\chi\|\bar{\mathbf{v}}\|\|\Phi_1\| + k(t)\chi\|\bar{\mathbf{v}}\|\|\Phi_2\| + \chi\|\bar{\mathbf{v}}\|\|\Phi_3\|\\ &+\|\mathbf{x}-\mathbf{x}_t^*\|\|\dot{\mathbf{x}}_t^*-\dot{\mathbf{r}}(t)\| + |\dot{\delta}(t)|\|\bar{\mathbf{v}}\|\|\mathbf{x}_t^*-\mathbf{r}(t)\|.\end{aligned} \tag{83}$$

Since $\|\mathbf{x}-\mathbf{x}_t^*\|\|\bar{\mathbf{v}}\|\leq\frac{\delta(t)k_1}{4}\|\mathbf{x}-\mathbf{x}_t^*\|^2 + \frac{1}{\delta(t)k_1}\|\bar{\mathbf{v}}\|^2$, $k_1(\delta(t)(\sqrt{N}\max_{i\in\mathcal{N}}\{l_i\}+\delta(t))+|\dot{\delta}(t)|)\|\mathbf{x}-\mathbf{x}_t^*\|\|\bar{\mathbf{v}}\|\leq\frac{\delta(t)k_1}{4}\|\mathbf{x}-\mathbf{x}_t^*\|^2 + \frac{k_1(\delta(t)(\sqrt{N}\max_{i\in\mathcal{N}}\{l_i\}+\delta(t))+|\dot{\delta}(t)|)^2}{\delta(t)}\|\bar{\mathbf{v}}\|^2$, $k_1(\max_{i\in\mathcal{N}}\{l_i\}+2\sqrt{N}\|\mathcal{P}\|(\sqrt{N}\max_{i\in\mathcal{N}}\{l_i\}+\delta(t)))\|\mathbf{x}-\mathbf{x}_t^*\|\|\bar{\mathbf{y}}\|\leq\frac{\delta(t)k_1}{4}\|\mathbf{x}-\mathbf{x}_t^*\|^2 + \frac{k_1(\max_{i\in\mathcal{N}}\{l_i\}+2\sqrt{N}\|\mathcal{P}\|(\sqrt{N}\max_{i\in\mathcal{N}}\{l_i\}+\delta(t)))^2}{\delta(t)}\|\bar{\mathbf{y}}\|^2$, $2\sqrt{N}\|\mathcal{P}\|\|\bar{\mathbf{v}}\|\|\bar{\mathbf{y}}\|\leq\frac{N\|P\|^2}{k_1}\|\bar{\mathbf{y}}\|^2 + k_1\|\bar{\mathbf{v}}\|^2$, $k_1(\omega(t)b+\delta(t)\max_{i\in\mathcal{N}}\{l_i\})\|\bar{\mathbf{v}}\|\|\bar{\mathbf{y}}\|\leq\frac{k_1(\omega(t)b+\delta(t)\max_{i\in\mathcal{N}}\{l_i\})^2}{2}\|\bar{\mathbf{v}}\|^2 + \frac{k_1}{2}\|\bar{\mathbf{y}}\|^2$, $2\sqrt{N}\|\mathcal{P}\|\chi\|\bar{\mathbf{y}}\|\|\Phi_2\|\leq\|\bar{\mathbf{y}}\|^2 + N\|\mathcal{P}\|^2\chi^2\|\Phi_2\|^2$, $k(t)\delta(t)k_1\chi\|\bar{\mathbf{v}}\|\|\Phi_1\|\leq\frac{k(t)}{4}\|\bar{\mathbf{v}}\|^2 + k(t)k_1^2\delta^2(t)\chi^2\|\Phi_1\|^2$, $k(t)\chi\|\bar{\mathbf{v}}\|\|\Phi_2\|\leq\frac{k(t)}{2}\|\bar{\mathbf{v}}\|^2 + \frac{k(t)\chi^2}{2}\|\Phi_2\|^2$ and $\chi\|\bar{\mathbf{v}}\|\|\Phi_3\|\leq\frac{\delta(t)k_1}{2}\|\bar{\mathbf{v}}\|^2 + \frac{\chi^2}{2\delta(t)k_1}\|\Phi_3\|^2$, one has

$$\begin{aligned}\dot{V} \overset{a.e.}{\leq} &-\frac{\delta(t)k_1}{4}\|\mathbf{x}-\mathbf{x}_t^*\|^2 - \kappa_1(t)\|\bar{\mathbf{v}}\|^2 - \kappa_2(t)\|\bar{\mathbf{y}}\|^2\\ &-\kappa_3(t)\|\Phi_1\|^2 - \kappa_4(t)\|\Phi_2\|^2 - \kappa_5(t)\|\Phi_3\|^2\\ &+\|\mathbf{x}-\mathbf{x}_t^*\|\|\dot{\mathbf{x}}_t^*-\dot{\mathbf{r}}(t)\| + |\dot{\delta}(t)|\|\bar{\mathbf{v}}\|\|\mathbf{x}_t^*-\mathbf{r}(t)\|\end{aligned}$$

where $\kappa_1(t) = \frac{k(t)}{4} - k_1 - \frac{1}{\delta(t)k_1} - \frac{3\delta(t)k_1}{2} - \frac{k_1(\delta(t)(\sqrt{N}\max_{i\in\mathcal{N}}\{l_i\}+\delta(t))+|\dot{\delta}(t)|)^2}{\delta(t)} - \frac{k_1(\omega(t)b+\delta(t)\max_{i\in\mathcal{N}}\{l_i\})^2}{2}$, $\kappa_2(t) = \omega(t)\lambda_{\min}(\mathcal{Q}) - 2k_1\sqrt{N}\|\mathcal{P}\|\max_{i\in\mathcal{N}}\{l_i\} - \frac{N\|P\|^2}{k_1} - \frac{k_1}{2} - 1 - \frac{k_1(\max_{i\in\mathcal{N}}\{l_i\}+2\sqrt{N}\|\mathcal{P}\|(\sqrt{N}\max_{i\in\mathcal{N}}\{l_i\}+\delta(t)))^2}{\delta(t)}$, $\kappa_3(t) = \alpha(t) - k(t)k_1^2\delta^2(t)\chi^2$,$\kappa_4(t) = \beta(t) - N\|\mathcal{P}\|^2\chi^2 - \frac{k(t)\chi^2}{2}$, and $\kappa_5(t) = \iota(t) - \frac{\chi^2}{2\delta(t)k_1}$. Choose $\omega(t)$, $k(t)$, $\alpha(t)$, $\beta(t)$, and $\iota(t)$ such that $\frac{\delta(t)k_1}{4} \leq \kappa_1(t)$, $\frac{\delta(t)k_1}{4} \leq \kappa_2(t)$, $\frac{\delta(t)k_1}{4} \leq \kappa_3(t)$, $\frac{\delta(t)k_1}{4} \leq \kappa_4(t)$, and $\frac{\delta(t)k_1}{4} \leq \kappa_5(t)$. Then, it can be derived that

$$\begin{aligned}\dot{V} \overset{a.e.}{\leq} & -\frac{\delta(t)k_1}{4}\|\mathbf{E}_5\|^2 + \|\mathbf{x} - \mathbf{x}_t^*\|\|\dot{\mathbf{x}}_t^* - \dot{\mathbf{r}}(t)\| \\ & + |\dot{\delta}(t)|\|\bar{\mathbf{v}}\|\|\mathbf{x}_t^* - \mathbf{r}(t)\|. \end{aligned} \tag{84}$$

The remaining analysis follows that proof of Theorem 3 and hence, is omitted here.

*Remark 9:* By Theorems 1–4 and Corollaries 2–4, it can be seen that both formation of the desired shape and distance optimization can be achieved when $t \to \infty$. This article discusses the least-distance formation tracking problem, where the target is moving around. If $r(t) = \mathbf{0}_m$, the proposed protocols can be reduced to address the least-distance formation problem [25], [26].

*Remark 10:* From Theorems 1–4 and Corollaries 2–4, it can be seen that the proposed algorithms can effectively achieve the least-distance formation tracking control. In comparison with the existing works, the proposed methods have the following advantages.

1) Different from [15], [16], [17], [18], [19], [20], [21], [22], [23], and [24] that consider predefined offsets between agents and the target, this article solves the least-distance formation tracking problem, in which the offsets are not predefined but determined by a global optimization problem.
2) In comparison with [25], [26], [27], and [28] that consider time-invariant optimization problems, this article allows the optimization problem to be time-varying and hence, the target can be moving around.
3) Though the method in [29] can deal with time-varying optimization problems with a formation constraint, only an approximated solution can be derived by adopting a large penalty parameter, which implies that there has a tradeoff between formation and tracking of a moving target with an optimal distance. However, the proposed methods in this article can ensure that formation and tracking of a moving target with an optimal distance can be simultaneously achieved. Besides, it is required that each agent can access the information of the target in [29], which is relaxed by the methods proposed in this article.

*Remark 11:* Note that first-order integrator-type systems and second-order integrator-type systems can effectively model velocity-actuated vehicles and acceleration-actuated vehicles, respectively. Moreover, many practical autonomous systems, such as surface vessels, aerial vehicles, and satellites, can also be reduced to second-order integrator-type systems [17], [51], [52]. Hence, the proposed method can be applied to deal with formation tracking in these systems. In addition, it is worth mentioning that for systems with controllable nonlinear dynamical systems, the modular framework [38] can be adopted to achieve least-distance formation tracking by using the proposed methods. In particular, one can use the proposed method to generate a trajectory that is convergent to the least-distance formation tracking solution and then, design a state regulator to deal with the nonlinear dynamics such that the actual state can track the trajectory generated by the proposed method. Therefore, the proposed least-distance formation tracking methods lay a solid foundation for applications in these nonlinear dynamical systems.

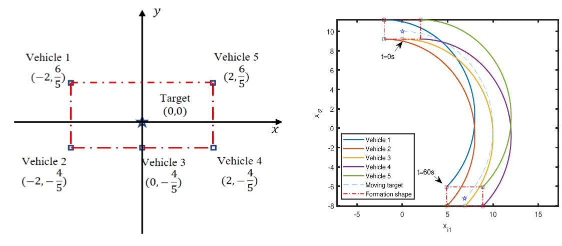

(a) (b)

Fig. 2. (a) Desired formation shape of the vehicles when the target is at the origin. (b) Desired trajectories of vehicles.

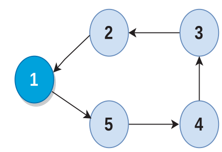


Fig. 3. Strongly connected digraph for vehicles.

## V. Simulation

In this section, simulations on acceleration-actuated vehicles and quadrotors are, respectively, presented to show the effectiveness of the proposed methods. In addition, some comparative simulations are provided to highlight the advantages of the proposed methods in comparison with existing methods.

### A. Acceleration-Actuated Vehicles

Consider a network of five mobile vehicles involved in the least-distance formation tracking game. To drive the positions of the vehicles to form the desired shape, it is set that $o_{ij} = 1 \quad \forall i \neq j$. Moreover, $d_1 = [0,0]^T$, $d_2 = [0,-2]^T$, $d_3 = [2,-2]$, $d_4 = [4,-2]$, and $d_5 = [4,0]^T$. It is computed that for each $r_x, r_y \in \mathbb{R}$, $x_1 = [r_x - 2, r_y + 2]^T$, $x_2 = [r_x - 2, r_y]^T$, $x_3 = [r_x, r_y]^T$, $x_4 = [r_x + 2, r_y]^T$, and $x_5 = [r_x + 2, r_y + 2]^T$ constitute a Nash equilibrium of the game (9).

For the formation tracking problem, the moving target is set as $r(t) = [r_1(t), r_2(t)]^T = [10\sin(\sigma t), 10\cos(\sigma t)]^T \in \mathbb{R}^2$, where $\sigma = 4\pi \times 10^{-2.5}$. Moreover, the least-norm Nash equilibrium is calculated as $\mathbf{x}_m^* = [-2, \frac{6}{5}, -2, -\frac{4}{5}, 0, -\frac{4}{5}, 2, -\frac{4}{5}, 2, \frac{6}{5}]^T$. Thus, the Nash equilibrium $\mathbf{x}^*(t) = [(x_1^*(t))^T, (x_2^*(t))^T, (x_3^*(t))^T, (x_4^*(t))^T, (x_5^*(t))^T]^T$, where $x_1^*(t) = [-2 + r_1(t), \frac{6}{5} + r_2(t)]^T$, $x_2^*(t) = [-2 + r_1(t), -\frac{4}{5} + r_2(t)]^T$, $x_3^*(t) = [r_1(t), -\frac{4}{5} + r_2(t)]^T$, $x_4^*(t) = [2 + r_1(t), -\frac{4}{5} + r_2(t)]^T$, $x_5^*(t) = [2 + r_1(t), \frac{6}{5} + r_2(t)]^T$. Correspondingly, Fig. 2(a) shows the desired formation shape when the moving target is at origin and Fig. 2(b) shows the desired trajectories of agents. In the upcoming simulations, vehicles exchange information via a strongly connected directed communication graph shown in Fig. 3. It is set that $a_{ij} = 1$ if agent $i$ can receive the information from agent $j$. In the following, least-distance formation tracking of acceleration-actuated vehicles will be presented.

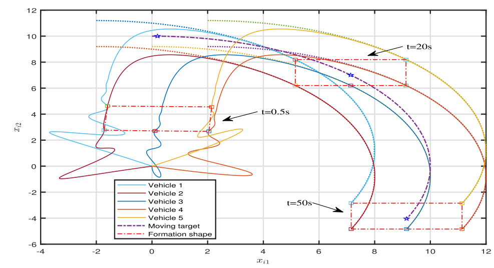


Fig. 4. Solid lines represent the actual trajectories of the vehicles generated by (47)–(48). The dotted lines represent the desired trajectories of the vehicles.

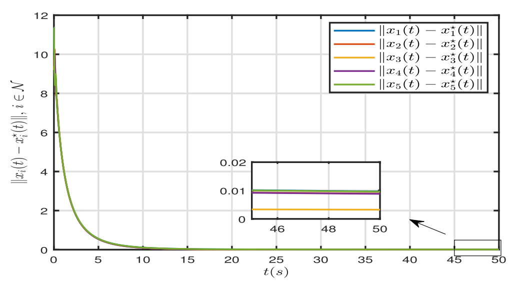


Fig. 5. Trajectory of $\|x_i(t) - x_i^*(t)\|$ for $i \in \mathcal{N}$, generated by (47)–(48).

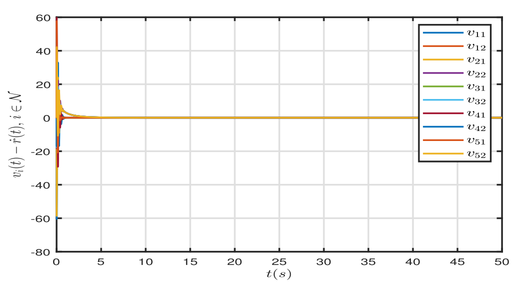


Fig. 6. Trajectories of $v_i(t) - \dot{r}(t)$ for $i \in \{1, 2, \ldots, 5\}$ generated by (47)–(48).

The dynamics of acceleration-actuated vehicles can be described by

$$\dot{x}_i(t) = v_i(t),\ \dot{v}_i(t) = u_i(t) \tag{85}$$

where $v_i(t) = [v_{i1}(t), v_{i2}(t)]^T \in \mathbb{R}^2$ is the velocity vector of vehicle $i$ and $u_i(t) = [u_{i1}(t), u_{i2}(t)]^T \in \mathbb{R}^2$ is the acceleration input.

***1) Information of the Moving Target is Available to All the Agents:*** In the simulation, it is set that $k_1 = 6$, $\delta(t) = 0.1(1+t)^{-0.4}$, $\omega(t) = 100 + 50(1+t)^{0.5}$, and $k(t) = 200 + 50(1+t)^{0.5}$. Simulation results generated by (47)–(48) are shown in Figs. 4–6 with the variables initialized at zero. Fig. 4 shows the position trajectories of the vehicles. Fig. 5 shows the trajectories of $\|x_i(t) - x_i^*(t)\|$, for $i \in \mathcal{N}$. Fig. 6 shows the trajectories of $v_i(t) - \dot{r}(t)$ for $i \in \{1, 2, \ldots, 5\}$. It can be clearly seen that the vehicles' velocities are convergent to $\dot{r}(t)$. These simulation results verify that vehicles can eventually achieve the least-distance formation tracking by utilizing the proposed method.

***2) Information of the Moving Target is Available to Only a Subset of the Agents:*** In the simulation, it is assumed that vehicle 1 can receive the information of the moving target, i.e., $\eta_1 = 1$ and $\eta_i = 0$, for $i \in \{2, 3, 4, 5\}$. Moreover, it is set that $k_1 = 6$, $\delta(t) = 0.1(1+t)^{-0.4}$, $\omega(t) = 50 + 100(1+t)^{0.5}$, $k(t) = 200 + 50(1+t)^{0.5}$, $\alpha(t) = 20$, $\beta(t) = 20 + 5(1+t)^{0.5}$, and $\iota(t) = 50 + 2(1+t)^{0.5}$. Simulation results generated by (72)–(73) are shown in Figs. 7–10 with the variables initialized at zero. From Fig. 7, it can be seen that the vehicles' estimates can converge to their actual values $r(t)$, $\dot{r}(t)$, and $\ddot{r}(t)$. Fig. 8 shows the vehicles' trajectories and

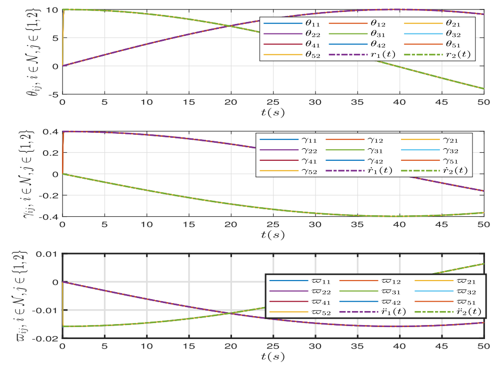


Fig. 7. Trajectories of $\theta_i(t)$, $\gamma_i(t)$, and $\varpi_i(t)$ for $i \in \{1, 2, \ldots, 5\}$ generated by (73).

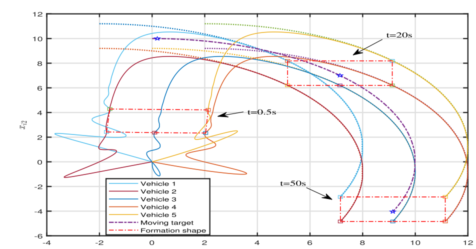


Fig. 8. Solid lines represent the actual trajectories of the vehicles generated by (72)–(73). The dotted lines represent the desired trajectories of the vehicles.

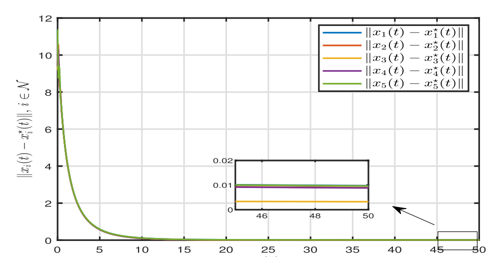


Fig. 9. Trajectories of $\|x_i(t) - x_i^*(t)\|$ for $i \in \mathcal{N}$, generated by (72)–(73).

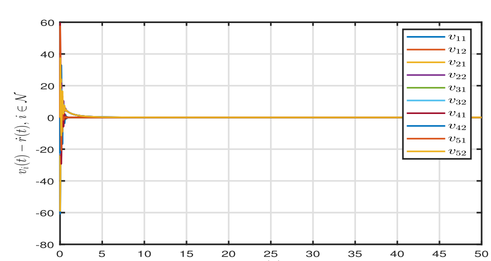


Fig. 10. Trajectories of $v_i(t) - \dot{r}(t)$ for $i \in \{1, 2, \ldots, 5\}$ generated by (72)–(73).

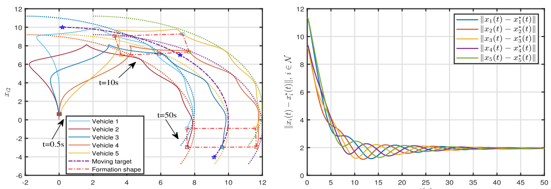


(a) (b)

Fig. 11. (a) Trajectories of the vehicles generated by the method in [28]. (b) Trajectories of $\|x_i(t) - x_i^*(t)\|$ for $i \in \mathcal{N}$, generated by the method in [28].

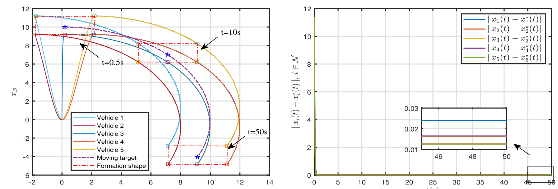


(a) (b)

Fig. 12. (a) Trajectories of the vehicles generated by the method in [29]. (b) Trajectories of $\|x_i(t) - x_i^*(t)\|$ for $i \in \mathcal{N}$, generated by the method in [29].

Fig. 9 shows $\|x_i(t) - x_i^*(t)\|$, for $i \in \mathcal{N}$. Fig. 10 shows the trajectories of $v_i(t) - \dot{r}(t)$ for $i \in \{1, 2, \ldots, 5\}$. It can be clearly seen that the vehicles' velocities are convergent to $\dot{r}(t)$. These simulation results verify that vehicles can eventually achieve the least-distance formation tracking by utilizing the proposed method.

## B. Comparison With Existing Methods

To further illustrate the advantages of the proposed methods, the methods in [28] and [29] are simulated as comparisons by focusing their ideas on achieving optimal formation control (accommodation of unknown Euler-Lagrange dynamics therein is not considered). Note that in the simulation, $d_i$ and $r(t)$ are the same as those in Section V-A.

By using the method in [28], one has

$$u_i = -k_3 v_i - (x_i - r(t)) - \sum_{j \in \mathcal{N}} a_{ij}(x_i - x_j) - \mu_i \quad \forall i \in \mathcal{N} \tag{86}$$

where $k_3$ is a positive constant and $\mu_i$ is generated by

$$\dot{\mu}_i = \sum_{j \in \mathcal{N}} a_{ij} \left( x_i - x_j + v_i - v_j - d_i + d_j \right). \tag{87}$$

By setting $k_3 = 5$, the simulation results of (86)–(87) are shown in Fig. 11 with all variables initialized at zero. From Fig. 11, it is not hard to find that though agents can maintain the desired formation shape, they cannot accurately track the moving target. Fig. 11(b) reveals that there is a gap between the actual trajectories and the desired trajectories of the agents.

Moreover, by using the method in [29], one has

$$\begin{aligned} u_i = & -k_5 \Bigg( k_4 \Bigg( (x_i - r(t)) + \beta_p \sum_{j=1}^{N} a_{ij}(x_i - x_j - d_i + d_j) \Bigg) \\ & + (v_i - \dot{r}(t)) + \beta_p \sum_{j=1}^{N} a_{ij}(v_i - v_j) \Bigg) \quad \forall i \in \mathcal{N} \end{aligned} \tag{88}$$

where $k_4, k_5, \beta_p$ are positive constants. Letting $k_4 = 2$, $\beta_p = 100$, and $k_5 = 60$, the simulation results of (88) are shown in Fig. 12 with all variables initialized at zero. Fig. 12 shows that (88) can achieve least-distance formation tracking with some steady-state error. Comparing Fig. 12(b) with Fig. 5, one can find that the steady-state errors generated by (88) are larger. The main reason is that [29] adopts penalty-based methods to achieve a tradeoff between formation tracking and global optimization, and hence, only an approximated result can be obtained with the given finite penalty parameter.

In addition to the above simulation results, it is worth pointing out that the methods in [28] and [29] require each agent to access the information of the target, which is relaxed by the methods proposed in this article.

## C. Applications for Multiple Quadrotors

In the following, least-distance formation tracking control among multiple quadrotors is considered.

It is considered that a network of five quadrotors is involved in the least-distance formation tracking game. The dynamics of each quadrotor $i$ can be described as [53]

$$\begin{bmatrix} M_i(x_i)\ddot{x}_i + C_i(x_i, \dot{x}_i)\dot{x}_i + G_i(x_i) \\ \bar{M}_i(\digamma_i)\ddot{\digamma}_i + \bar{C}_i(\digamma_i, \dot{\digamma}_i)\dot{\digamma}_i + \bar{G}_i(\digamma_i) \end{bmatrix} = \begin{bmatrix} \tau_i \\ N_i \end{bmatrix} \tag{89}$$

for $i \in \mathcal{N}$, where $x_i = [x_{i1}, x_{i2}, x_{i3}]^T \in \mathbb{R}^3$ represents the position of each quadrotor and $\digamma_i = [roll_i, pitch_i, yaw_i]^T \in \mathbb{R}^3$ represents the roll, pitch, and yaw angles of quadrotor $i$, $M_i(x_i) = \varsigma_i I_3$ ($\varsigma_i$ is the mass of quadrotor $i$), $C_i(x_i, \dot{x}_i) = \mathbf{0}_{3\times3}$ ($\mathbf{0}_{3\times3}$ represents $3 \times 3$ dimensional zero matrix), $G_i(x_i) = \varsigma_i[0, 0, g]^T$, $\varsigma_i = 2kg$, and $g = 9.8m/s^2$ is the gravity acceleration. Moreover, $\bar{M}_i(\digamma_i)$, $\bar{C}_i(\digamma_i, \dot{\digamma}_i)$ and $\bar{G}_i(\digamma_i)$ can be found in [53]. In addition, $\tau_i$ and $N_i$ are the external force and torque, respectively.

In the simulation, it is set that $o_{ij} = 1, \quad \forall i \neq j$. Moreover, $d_1 = [0, 0, 0]^T$, $d_2 = [0, -2, 0]^T$, $d_3 = [2, -2, 0]^T$, $d_4 = [4, -2, 0]^T$, and $d_5 = [4, 0, 0]^T$. Moreover, the moving target is set as $r(t) = [r_1(t), r_2(t), r_3(t)]^T = [10\sin(\sigma t), 10\cos(\sigma t), t]^T \in \mathbb{R}^3$. Thus, the Nash equilibrium is $\mathbf{x}^*(t) = [(x_1^*(t))^T, (x_2^*(t))^T, (x_3^*(t))^T, (x_4^*(t))^T, (x_5^*(t))^T]^T$, where $x_1^*(t) = [-2 + r_1(t), \frac{6}{5} + r_2(t), r_3(t)]^T$, $x_2^*(t) = [-2 + r_1(t), -\frac{4}{5} + r_2(t), r_3(t)]^T$, $x_3^*(t) = [r_1(t), -\frac{4}{5} + r_2(t), r_3(t)]^T$, $x_4^*(t) = [2 + r_1(t), -\frac{4}{5} + r_2(t), r_3(t)]^T$, $x_5^*(t) = [2 + r_1(t), \frac{6}{5} + r_2(t), r_3(t)]^T$.

In the following simulation, these quadrotors exchange their information via Fig. 3. In addition, an *inner–outer loop control scheme* [17] is utilized to achieve the least-distance formation tracking for quadrotors. The inner loop controller is adopted from [26]. In addition, by following [26], the outer loop controller $\tau_i$ can be designed as

$$\tau_i = M_i(x_i)u_i + G_i(x_i) \tag{90}$$

for $i \in \mathcal{N}$, where $u_i$ is given in (72). Moreover, the choices of $k_1$, $\delta(t)$, $k(t)$, $\omega(t)$, $\alpha(t)$, $\gamma(t)$, and $\iota(t)$ and initial state settings are the same as those in Section V-A2. Then, simulation results are shown in Figs. 13–14. Fig. 13 shows the position trajectories of the quadrotors, from which it is clear that the least-distance formation tracking can be achieved. Fig. 14 shows the trajectories of attitudes of quadrotors, which implies that the attitudes can be stabilized. These results verify the effectiveness of the proposed scheme.

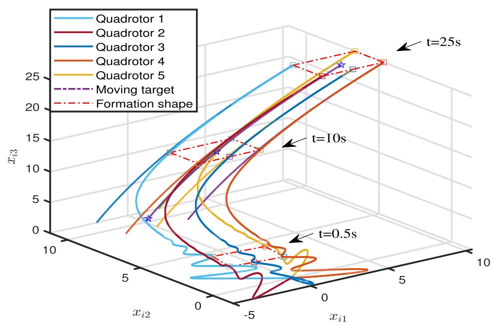


Fig. 13. Solid lines represent the actual trajectories of the quadrotors generated by (72)–(73) and (90). The dotted lines represent the desired trajectories of the quadrotors.

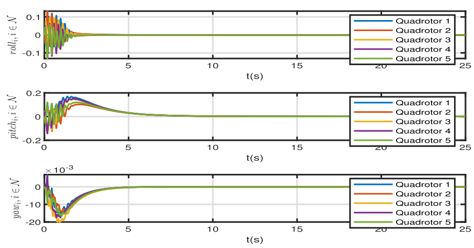


Fig. 14. Trajectories of roll, pitch, and yaw angles generated by the method in [26].

## VI. Conclusion

In this article, the least-distance formation tracking problem has been solved by utilizing a game-based method. Protocols for first-order and second-order integrator-type agents have been successively investigated. For both systems, the cases in which the trajectory information of the moving target is known to all agents and known to only a subset of agents have been addressed. By utilizing consensus protocols, regularization techniques and gradient optimization algorithms, least-distance formation tracking strategies have been established. It has been theoretically proven that least-distance formation tracking can be achieved by using the developed strategies. Future works will take time-varying optimal formation control and security issues into consideration.

## References


[1] Y. Dong and J. Huang, "A leader-following rendezvous problem of double integrator multi-agent systems," *Automatica*, vol. 49, no. 5, pp. 1386–1391, 2013.

[2] Y. Yuan, Y. Wang, and L. Guo, "Sliding-mode-observer-based time-varying formation tracking for multispacecrafts subjected to switching topologies and time-delays," *IEEE Trans. Autom. Control*, vol. 66, no. 8, pp. 3848–3855, Aug. 2021.

[3] Z. Lin, L. Wang, Z. Han, and M. Fu, "Distributed formation control of multi-agent systems using complex laplacian," *IEEE Trans. Autom. Control*, vol. 59, no. 7, pp. 1765–1777, Jul. 2015.

[4] C. Deng, C. Wen, W. Wang, X. Li, and D. Yue, "Distributed adaptive tracking control for high-order nonlinear multi-agent systems over event-triggered communication," *IEEE Trans. Autom. Control*, vol. 68, no. 2, pp. 1176–1183, Feb. 2024.

[5] Z. Zhang, S. Chen, and Y. Zheng, "Fully distributed scaled consensus tracking of high-order multiagent systems with time delays and disturbances," *IEEE Trans. Ind. Inform.*, vol. 18, no. 1, pp. 305–314, Jan. 2022.

[6] J. Shao, W. X. Zheng, L. Shi, and Y. Cheng, "Leader-follower flocking for discrete-time Cucker-Smale models with lossy links and general weight functions," *IEEE Trans. Autom. Control*, vol. 66, no. 10, pp. 4945–4951, Oct. 2020.

[7] Z. S. Lippay and J. B. Hoagg, "Formation control with time-varying formations, bounded controls, and local collision avoidance," *IEEE Trans. Control Syst. Technol.*, vol. 30, no. 1, pp. 261–276, Jan. 2022.

[8] X. Jin, Y. Tang, Y. Shi, W. Zhang, and W. Du, "Event-triggered formation control for a class of uncertain Euler-Lagrange systems: Theory and experiment," *IEEE Trans. Control Syst. Technol.*, vol. 30, no. 1, pp. 336–343, Jan. 2022.

[9] H. Liu, T. Ma, F. L. Lewis, and Y. Wan, "Robust formation trajectory tracking control for multiple quadrotors with communication delays," *IEEE Trans. Control Syst. Technol.*, vol. 28, no. 6, pp. 2633–2640, Jun. 2020.

[10] J. Han and Y. Chen, "Multiple UAV formations for cooperative source seeking and contour mapping of a radiative signal field," *J. Intell. Robotic Syst.*, vol. 74, pp. 323–332, 2014.

[11] R. Ringbäck, J. Wei, E. S. Erstorp, J. Kuttenkeuler, T. A. Johansen, and K. H. Johansson, "Multi-agent formation tracking for autonomous surface vehicles," *IEEE Trans. Control Syst. Technol.*, vol. 29, no. 6, pp. 2287–2298, Jun. 2020.

[12] X. Ge and Q.-L. Han, "Distributed formation control of networked multi-agent systems using a dynamic event-triggered communication mechanism," *IEEE Trans. Ind. Electron.*, vol. 64, no. 10, pp. 8118–8127, Oct. 2017.

[13] G. Bower, T. Flanzer, and I. Kroo, "Formation geometries and route optimization for commercial formation flight," in *Proc. 27th AIAA Appl. Aerodynamics Conf.*, 2009, p. 3615.

[14] T. Balch and R. C. Arkin, "Behavior-based formation control for multirobot teams," *IEEE Trans. Robot. Autom.*, vol. 14, no. 6, pp. 926–939, Jun. 1998.

[15] J. Wang, L. Han, X. Dong, Q. Li, and Z. Ren, "Distributed sliding mode control for time-varying formation tracking of multi-UAV system with a dynamic leader," *Aerosp. Sci. Technol.*, vol. 111, 2021, Art. no. 106549.

[16] C.-D. Liang, M.-F. Ge, Z.-W. Liu, G. Ling, and F. Liu, "Predefined-time formation tracking control of networked marine surface vehicles," *Control Eng. Pract.*, vol. 107, 2021, Art. no. 104682.

[17] X. Dong, Y. Zhou, Z. Ren, and Y. Zhong, "Time-varying formation tracking for second-order multi-agent systems subjected to switching topologies with application to quadrotor formation flying," *IEEE Trans. Ind. Electron.*, vol. 64, no. 6, pp. 5014–5024, Jun. 2016.

[18] J. Hu, P. Bhowmick, and A. Lanzon, "Distributed adaptive time-varying group formation tracking for multiagent systems with multiple leaders on directed graphs," *IEEE Trans. Control Netw. Syst.*, vol. 7, no. 1, pp. 140–150, Jan. 2019.

[19] C. Viel, S. Bertrand, M. Kieffer, and H. Piet-Lahanier, "Distributed event-triggered control strategies for multi-agent formation stabilization and tracking," *Automatica*, vol. 106, pp. 110–116, 2019.

[20] W. Wang, J. Huang, C. Wen, and H. Fan, "Distributed adaptive control for consensus tracking with application to formation control of nonholonomic mobile robots," *Automatica*, vol. 50, no. 4, pp. 1254–1263, 2014.

[21] M.-F. Ge, Z.-H. Guan, C. Yang, T. Li, and Y.-W. Wang, "Time-varying formation tracking of multiple manipulators via distributed finite-time control," *Neurocomputing*, vol. 202, pp. 20–26, 2016.

[22] Z. Wang, Y. Zou, Y. Liu, and Z. Meng, "Distributed control algorithm for leader–follower formation tracking of multiple quadrotors: Theory and experiment," *IEEE/ASME Trans. Mechatron.*, vol. 26, no. 2, pp. 1095–1105, Feb. 2020.

[23] H. Liu, Y. Wang, F. L. Lewis, and K. P. Valavanis, "Robust formation tracking control for multiple quadrotors subject to switching topologies," *IEEE Trans. Control Netw. Syst.*, vol. 7, no. 3, pp. 1319–1329, Mar. 2020.

[24] Y. Hua, X. Dong, G. Hu, Q. Li, and Z. Ren, "Distributed time-varying output formation tracking for heterogeneous linear multiagent systems with a nonautonomous leader of unknown input," *IEEE Trans. Autom. Control*, vol. 64, no. 10, pp. 4292–4299, Oct. 2019.

[25] L. Ding, M. Ye, Q.-L. Han, and G. Jia, "Distributed Nash equilibrium seeking in merely monotone games using an event- and switching-activated communication scheme," *IEEE Trans. Autom. Control*, vol. 70, no. 1, pp. 471–478, Jan. 2025.

[26] J. Shi, M. Ye, L. Ding, and S. Xu, "Distributed least-distance formation control for Euler-Lagrange systems: A game-based approach," *Control Eng. Pract.*, vol. 142, 2024, Art. no. 105743.

[27] J. Shi and M. Ye, "Distributed optimal formation control for unmanned surface vessels by a regularized game-based approach," *IEEE/CAA J. Automatica Sinica*, vol. 11, no. 1, pp. 276–278, Jan. 2024.

[28] L. Jiang, Z. Jin, and Z. Qin, "Distributed optimal formation for uncertain Euler-Lagrange systems with collision avoidance," *IEEE Trans. Circuits Syst. II: Exp. Briefs*, vol. 69, no. 8, pp. 3415–3419, Aug. 2022.

[29] C. Sun, Z. Feng, and G. Hu, “Time-varying optimization-based approach for distributed formation of uncertain Euler-Lagrange systems,” *IEEE Trans. Cybern.*, vol. 52, no. 7, pp. 5984–5998, Jul. 2021.

[30] L. Brinón-Arranz, A. Seuret, and C. Canudas-de Wit, “Cooperative control design for time-varying formations of multi-agent systems,” *IEEE Trans. Autom. Control*, vol. 59, no. 8, pp. 2283–2288, Aug. 2014.

[31] L. Dou, C. Song, X. Wang, L. Liu, and G. Feng, “Target localization and enclosing control for networked mobile agents with bearing measurements,” *Automatica*, vol. 118, 2020, Art. no. 109022.

[32] S. Ju, J. Wang, and L. Dou, “Enclosing control for multiagent systems with a moving target of unknown bounded velocity,” *IEEE Trans. Cybern.*, vol. 52, no. 11, pp. 11561–11570, Nov. 2021.

[33] X. Peng, K. Guo, and Z. Geng, “Moving target circular formation control of multiple non-holonomic vehicles without global position measurements,” *IEEE Trans. Circuits Syst. II: Exp. Briefs*, vol. 67, no. 2, pp. 310–314, Feb. 2019.

[34] M. S. Stankovic, K. H. Johansson, and D. M. Stipanovic, “Distributed seeking of Nash equilibria with applications to mobile sensor networks,” *IEEE Trans. Autom. Control*, vol. 57, no. 4, pp. 904–919, Apr. 2011.

[35] Z. Deng, “Game-based formation control of high-order multi-agent systems,” *IEEE Trans. Netw. Sci. Eng.*, vol. 10, no. 1, pp. 140–151, Jan. 2022.

[36] W. Lin, C. Li, Z. Qu, and M. A. Simaan, “Distributed formation control with open-loop Nash strategy,” *Automatica*, vol. 106, pp. 266–273, 2019.

[37] D. Gu, “A differential game approach to formation control,” *IEEE Trans. Control Syst. Technol.*, vol. 16, no. 1, pp. 85–93, Jan. 2007.

[38] M. Ye, Q.-L. Han, L. Ding, and S. Xu, “Distributed Nash equilibrium seeking in games with partial decision information: A survey,” *Proc. IEEE*, vol. 111, no. 2, pp. 140–157, Feb. 2023.

[39] K. Lu, G. Jing, and L. Wang, “Distributed algorithms for searching generalized Nash equilibrium of noncooperative games,” *IEEE Trans. Cybern.*, vol. 49, no. 6, pp. 2362–2371, Jun. 2018.

[40] X.-F. Wang, X.-M. Sun, A. R. Teel, and K.-Z. Liu, “Distributed robust Nash equilibrium seeking for aggregative games under persistent attacks: A hybrid systems approach,” *Automatica*, vol. 122, 2020, Art. no. 109255.

[41] G. Shao, X.-F. Wang, and R. Wang, “Distributed Nash equilibrium seeking of aggregative games under networked attacks,” *Asian J. Control*, vol. 24, no. 2, pp. 659–668, 2022.

[42] Y. Yuan, C. Ma, L. Guo, and P. Zhang, “Event-triggered Nash equilibrium seeking for multiagent systems with stubborn eso,” *IEEE Trans. Syst., Man, Cybern. Syst.*, vol. 53, no. 3, pp. 1347–1358, Mar. 2023.

[43] X. Nian, F. Niu, and Z. Yang, “Distributed Nash equilibrium seeking for multicluster game under switching communication topologies,” *IEEE Trans. Syst., Man, Cybern. Syst.*, vol. 52, no. 7, pp. 4105–4116, Jul. 2022.

[44] F. L. Lewis, H. Zhang, K. Hengster-Movric, and A. Das, *Cooperative Control of Multi-Agent Systems Optimal and Adaptive Design Approaches*. London, U.K.: Springer, 2014.

[45] M. Ye and G. Hu, “Distributed Nash equilibrium seeking by a consensus based approach,” *IEEE Trans. Autom. Control*, vol. 62, no. 9, pp. 4811–4818, Sep. 2017.

[46] F. Facchinei and J.-S. Pang, *Finite-Dimensional Variational Inequalities and Complementarity Problems*. Berlin, Germany: Springer, 2004.

[47] M. Ye, G. Hu, F. L. Lewis, and L. Xie, “A unified strategy for solution seeking in graphical $n$-coalition noncooperative games,” *IEEE Trans. Autom. Control*, vol. 64, no. 11, pp. 4645–4652, Nov. 2019.

[48] R. Cominetti, J. Peypouquet, and S. Sorin, “Strong asymptotic convergence of evolution equations governed by maximal monotone operators with Tikhonov regularization,” *J. Differ. Equ.*, vol. 245, no. 12, pp. 3753–3763, 2008.

[49] R. I. Boţ, S.-M. Grad, D. Meier, and M. Staudigl, “Inducing strong convergence of trajectories in dynamical systems associated to monotone inclusions with composite structure,” *Adv. Nonlinear Anal.*, vol. 10, no. 1, pp. 450–476, 2020.

[50] M. Ye, L. Ding, Q.-L. Han, J. Shi, and C. Shen, “Distributed optimal formation tracking of multiple noncooperative targets: A time-varying game-based approach,” *Automatica*, vol. 173, 2024, Art. no. 112074.

[51] B.-B. Hu, H.-T. Zhang, and J. Wang, “Multiple-target surrounding and collision avoidance with second-order nonlinear multiagent systems,” *IEEE Trans. Ind. Electron.*, vol. 68, no. 8, pp. 7454–7463, Aug. 2021.

[52] D. Li, W. Zhang, W. He, C. Li, and S. S. Ge, “Two-layer distributed formation-containment control of multiple Euler-Lagrange systems by output feedback,” *IEEE Trans. Cybern.*, vol. 49, no. 2, pp. 675–687, Feb. 2019.

[53] K. Guo, J. Jia, X. Yu, L. Guo, and L. Xie, “Multiple observers based anti-disturbance control for a quadrotor UAV against payload and wind disturbances,” *Control Eng. Pract.*, vol. 102, 2020, Art. no. 104560.


**Jun Shi** received the B.Eng. degree in automation from Changzhou University, Jiangsu, China, in 2021. He is currently working toward the Ph.D. degree in control science and engineering with the School of Automation, Nanjing University of Science and Technology, Nanjing, China.

His current research interests include formation control, game theory, distributed optimization, and their applications.

**Maojiao Ye** (Senior Member, IEEE) received the B.Eng. degree in automation from the University of Electronic Science and Technology of China, Sichuan, China, in 2012 and the Ph.D. degree from Nanyang Technological University, Singapore, in 2016.

She is currently a Professor with the School of Automaton, Nanjing University of Science and Technology. Her research interests include game theory, distributed optimization, and their applications.

**Lei Ding** (Senior Member, IEEE) received the B.Eng. degree in automation, and the M.Eng. and Ph.D. degrees in control theory and control engineering from Dalian Maritime University, Dalian, China, in 2007, 2009, and 2014, respectively.

He is currently a Full Professor with the Nanjing University of Posts and Telecommunications, Nanjing, China. His research interests include cooperative control, distributed optimization, and game theory in networked systems and their applications to smart grids/microgrids.

**Shengyuan Xu** (Senior Member, IEEE) received the B.Sc. degree in mathematics from Hangzhou Normal University, Hangzhou, China, in 1990, the M.Sc. degree in operational research and cybernetics from Qufu Normal University, Qufu, China, in 1996, and the Ph.D. degree in control theory and control engineering from the Nanjing University of Science and Technology, Nanjing, China, in 1999.

He is currently a Professor with the School of Automation, Nanjing University of Science and Technology. His current research interests include robust filtering and control, singular systems, time-delay systems, neural networks, multidimensional systems, and nonlinear systems.

**Qing-Long Han** (Fellow, IEEE) received the B.Sc. degree in mathematics from Shandong Normal University, Jinan, China, in 1983, and the M.Sc. and Ph.D. degrees in control engineering from the East China University of Science and Technology, Shanghai, China, in 1992 and 1997, respectively.

He is Pro Vice-Chancellor (Research Quality) and a Distinguished Professor with Swinburne University of Technology, Melbourne, Australia. He held various academic and management positions with Griffith University and Central Queensland University, Australia. His research interests include networked control systems, multiagent systems, time-delay systems, smart grids, unmanned surface vehicles, and neural networks.